Molecular Pharmacology Fast Forward. Published on March 27, 2008 as doi:10.1124/mol.108.045591
This article has not been copyedited and formatted. The final version may differ from this version.

PROBING THE BINDING SITES AND MECHANISMS OF ACTION OF TWO hERG CHANNEL ACTIVATORS, NS1643 AND PD307243

Xulin Xu[1], Maurizio Recanatini[2], Marinella Roberti[2], Gea-Ny Tseng[1]

1. Department of Physiology

Virginia Commonwealth University

Richmond, VA

2. Department of Pharmaceutical Sciences

University of Bologna

Bologna, Italy

Molecular Pharmacology Fast Forward. Published on March 27, 2008 as DOI: 10.1124/mol.108.045591
This article has not been copyedited and formatted. The final version may differ from this version.

Running title: HERG activators, channel inactivation and selectivity filter

For correspondence:
Gea-Ny Tseng, PhD
Department of Physiology
Virginia Commonwealth University
1101 E. Marshall Street
Richmond, VA 23298
Phone: 804-827-0811
Fax: 804-828-7382
e-mail: gtseng@vcu.edu

Number of text pages: 40

Number of table(s): 1

Number of figures: 10

Number of references: 33

Number of words in the *Abstract*: 249

Number of words in the *Introduction*: 705

Number of words in the *Discussion*: 1495

Nonstandard abbreviations:

PD	=	PD307243
NS	=	NS1643
V_t	=	test pulse voltage
V_r	=	repolarization voltage
I_{f-a}	=	fully-activated current
-S-S-	=	disulfide bonded state
+MTS	=	treated by a methanethiosulfonate reagent
TPeA	=	tetrapentylammonium
DOF	=	dofetilide

Molecular Pharmacology Fast Forward. Published on March 27, 2008 as DOI: 10.1124/mol.108.045591
This article has not been copyedited and formatted. The final version may differ from this version.

ABSTRACT

We studied the mechanisms and sites of activator actions of PD(307243) and NS(1643) on the hERG channel expressed in oocytes and COS-7 cells. PD and NS affected hERG in a concentration-dependent manner, reaching a maximal increase in current amplitude by 100% and $\geq$ 300% (1-s test pulse to 0 mV), with apparent K_d values of 3 and 20 uM, respectively. Both drugs slowed hERG inactivation. NS additionally shifted the activation curve in the negative direction, accelerated activation and slowed deactivation. Kinetic model simulations suggested that the activator effects of PD and NS could be largely accounted for by their effects on the hERG gating kinetics. Both drugs worked from outside the cell membrane but their binding sites appeared to be distinctly different. Perturbing the conformation of outer vestibule/external pore entrance (by cysteine substitution at high-impact positions or cysteine side chain modification at intermediate-impact positions) prevented the activator effect of NS but not that of PD. Furthermore, a peptide toxin BeKm-1 that bound to the outer mouth of the hERG channel suppressed NS effect but potentiated PD effect. We propose that NS is a 'gating-modifier': it binds to the outer vestibule/pore entrance of hERG and increases current amplitudes by promoting channel activation while retarding inactivation. PD's activator effect was prevented by external quaternary ammonium cations or dofetilide, which approached the hERG selectivity filter from opposite sides of the membrane and depleted K^+ ions in the selectivity filter. We suggest that PD may work as a 'pore-modifier' of the hERG channel.

Molecular Pharmacology Fast Forward. Published on March 27, 2008 as DOI: 10.1124/mol.108.045591
This article has not been copyedited and formatted. The final version may differ from this version.

INTRODUCTION

The *human ether-a-go-go related gene* encodes the pore-forming component of the rapid delayed rectifier (I_{Kr}) channel (Sanguinetti *et al.*, 1995). The hERG/I_{Kr} channel is important for action potential repolarization in the heart (Tseng, 2001). Mutations in hERG/I_{Kr} have been linked to congenital long QT (LQT2) or short QT (SQT1) syndrome (Brugada *et al.*, 2004). A more common problem is the sensitivity of hERG/I_{Kr} channel to a wide range of drugs (Recanatini *et al.*, 2005). Unintentional drug blockade of hERG/I_{Kr} is the major cause for the acquired LQT syndrome (aLQT) (Roden, 2004). This problem has prompted the development of 'hERG activators' to combat aLQT, and perhaps LQT2. To achieve this goal, the hERG activators should be able to increase currents through the channel under a wide range of conditions: channel blockade by different chemicals as seen in aLQT, and channel malfunction due to various mutations as seen in LQT2. To design such robust hERG activators, knowledge about the mechanisms and sites of actions of available hERG activators is important.

Three major classes of hERG channel activators are available, represented by the following prototypes: RPR260243 (Kang *et al.*, 2005), NS1643 (Casis *et al.*, 2006; Hansen *et al.*, 2006) and PD118057 (Zhou *et al.*, 2005). The mechanism and site of action of RPR260243 have been elucidated recently. RPR260243 slows hERG channel deactivation (Kang *et al.*, 2005). Mutations of specific residues in the S4-S5 linker, cytoplasmic halves of S5 and S6 could attenuate or abolish the activator effect of RPR260243 (Perry *et al.*, 2007). Mapping these positions to the Kv1.2 crystal structure showed that they are close to each other in 3-D space, in a region critically involved in the voltage-dependent activation/deactivation gating processes (Long *et al.*, 2005). These observations provided a satisfying explanation for the pharmacological action of RPR260243.

Molecular Pharmacology Fast Forward. Published on March 27, 2008 as DOI: 10.1124/mol.108.045591
This article has not been copyedited and formatted. The final version may differ from this version.

A previous study on NS1643 suggested that this hERG activator mainly increased outward, but not inward, currents through the channels (Casis *et al*., 2006). Furthermore, mutations at the external pore entrance and in the pore loop that perturb the inactivation process of the hERG channel can attenuate the activator effect of NS1643. On the other hand, mutations of an aromatic residues (F656) on S6, that is critical for hERG blocker binding within the inner cavity (Kamiya *et al*., 2006), potentiate the activator effect of NS1643 (Casis *et al*., 2006). It was suggested that NS1643 works mainly by hindering channel inactivation. However, detailed analysis of the effects of NS1643 on hERG gating kinetics has been limited, so that the mechanism and site of its activator action are not entirely clear.

A previous study on PD118057 showed that this drug increased outward currents through the hERG channels with little effects on the voltage-dependence or kinetics of activation and deactivation (Zhou *et al*., 2005). PD118057 also slowed the rate of channel inactivation at 36^{o}C. A recent study on PD307243, a structure analog of PD118057, showed that this hERG activator could dramatically slow the rate of channel deactivation, to the extent that some of the channels became constitutively active at hyperpolarized voltages (Gordon *et al.*, 2008). The authors also reported that PD307243 greatly slowed the rate of hERG inactivation at depolarized voltages. A combination of these two effects created a transient outward current (I_{to})-like channel phenotype for the hERG channel (Gordon *et al*., 2008). There have been no mutagenesis experiments to probe for the binding site of PD118057 or PD307243 in the hERG channel. The mechanism for the peculiar pharmacological actions of PD307243 is not clear.

We undertook the present study to investigate the mechanisms and sites of activator actions of PD307243 and NS1643 (chemical structures shown in Zhou *et al.*, 2005, and Casis *et al*., 2006) . Experiments were designed to systematically address the following questions:

Molecular Pharmacology Fast Forward. Published on March 27, 2008 as DOI: 10.1124/mol.108.045591
This article has not been copyedited and formatted. The final version may differ from this version.

1. How do these drugs modify the gating kinetics of the hERG channel, and can the drug effects on channel gating account for their activator actions?
2. Is there a membrane 'sidedness' in the activators' actions? This information is needed for the design of the following experiments to probe for the drug binding sites.
3. How do perturbations of the outer vestibule and external pore entrance of the hERG channel impact on the activator actions of PD307243 and NS1643?
4. How do pore blockers from outside or inside the cell membrane impact on the activator actions of PD307243 and NS1643?

MATERIALS AND METHODS

1. Molecular biology

The hERG1 WT cDNA was a kind gift from Dr. Gail A. Robertson (Wisconsin University). The hERG cDNA was subcloned into a vector, pAlterMax, and site-specific cysteine (Cys) substitutions were made using the oligonucleotide-directed method and a commercial kit (Altered Site^{R} Mammalian Mutagenesis System, Promega) as described in our previous publications (Liu *et al*., 2002). Mutations were confirmed by DNA sequencing. Transcription of cRNAs was performed using the Mmessage Mmachine kit from Ambion. The concentrations and quality of cRNA products were examined using cRNA gel densitometry (ChemiImager Model 4000, α-Innotech) before oocyte injection.

2. Oocyte experiments

Oocytes were isolated as described previously (Liu *et al*., 2002). Each oocyte was microinjected with 40 nl of cRNA solution (total cRNA 10 - 18 ng). After cRNA injection,

Molecular Pharmacology Fast Forward. Published on March 27, 2008 as DOI: 10.1124/mol.108.045591
This article has not been copyedited and formatted. The final version may differ from this version.

oocytes were incubated in ND96 medium (in mM: NaCl 96, KCl 2, $CaCl_2$ 1.8, $MgCl_2$ 1, HEPES 5, Na-pyruvate 2.5, pH 7.5) supplemented with horse serum (4%) and antibiotics (penicillin 50 U/ml and streptomycin 50 U/ml) for 3- 5 days before experiments. Voltage clamp was performed using the '2-cushion pipette' methods (Schreibmayer *et al.*, 1994). Oocytes were superfused or bathed in a low [Cl]-ND96 solution (Cl^- ions in ND96 replaced by methanesulfonate, to minimize interference from oocyte endogenous Cl currents), and membrane currents were recorded using an Oocyte Clamp amplifier (model 725B or 725C, Warner Instruments). Voltage clamp protocol generation and data acquisition were controlled by pClamp 5.5 via computer and a 12-bit D/A and A/D converter (Axon Instruments).

3. **COS-7 experiments**

COS-7 cells were maintained in D-MEM (Gibco) supplemented with 10% fetal calf serum (Hyclone) and penicillin/streptomycin, in a moist 5% CO_2 chamber at 36^oC. Cells were plated at a sub-confluence level the day before transfection. Each 35-mm dish was added cDNAs for hERG (1 ug) and CD8 (0.2 ug), reaching cDNA molar ratio of 1:0.25. Currents were recorded 24-48 hr after transfection. Cells were exposed to CD8 mAb-coated beads (Dynal) at room temperature for 10 min, treated with trypsin-EDTA (Gibco) at room temperature for 5 min, and cell suspension was added to a poly-L-lysine coated coverslip placed in the cell chamber. Cells decorated with CD8-mAb beads were used for patch clamping. The pipette solution contained (mM): K-aspartate 115, KCl 20, EGTA 10, ATP(K salt) 10, $MgCl_2$ 1, and HEPES 10 (pH 7.3). Pipette tip resistance was 1.9 - 2.1 MΩ, and 95% of series resistance was compensated. The bath solution was normal Tyrode's (mM): NaCl 147, KCl 4, $CaCl_2$ 2, $MgCl_2$ 1, HEPES 5, and dextrose 5.5 (pH 7.3). Whole cell patch clamp was performed using AxoPatch 200B

Molecular Pharmacology Fast Forward. Published on March 27, 2008 as DOI: 10.1124/mol.108.045591
This article has not been copyedited and formatted. The final version may differ from this version.

controlled by pClamp10 via DigiData1440A. Methods of data analysis were similar to those described for oocyte experiments.

4. Guinea pig ventricular myocyte experiments

Myocytes were isolated from a young adult male guinea pig (375 g) using collagenase digestion followed by gentle mechanical trituration as described before (Yao *et al.*, 1999). Whole cell current recording conditions were similar to those described for COS-7 experiments, except: (1) during current recording, myocytes were superfused with a nominally Na- and Ca-free Tyrode's solution (NaCl and $CaCl_2$ replaced by equimolar choline-Cl and $MgCl_2$), and (2) recoding temperature was 33-34^{o}C. Guinea pig ventricular myocytes express a sizable I_{Kr} as well as a robust slow delayed rectifier current (I_{Ks}) (Sanguinetti and Jurkiewicz, 1990). However, we could not identify reagents or conditions that could selectively suppress I_{Ks} without affecting I_{Kr}, to allow a direct detection of agonist effects on I_{Kr}. Therefore, we relied on the difference in the voltage range of activation between I_{Kr} and I_{Ks} (Sanguinetti and Jurkiewicz1990). At 33-34^{o}C the most suitable voltage range for recording I_{Kr} (as a time-dependent outward current largely free of I_{Ks}) was -20 to -10 mV. Removing extracellular Na and Ca ions was necessary since this voltage range overlapped with those of Na and Ca channel currents.

5. **Data analysis and kinetic model simulations**

The voltage clamp protocols and methods of data analysis used to characterize the effects of PD307243 and NS1643 on voltage-dependence and rate of activation, deactivation and inactivation of the hERG channel are described in Fig. 1 and legend. Simulations of hERG

Molecular Pharmacology Fast Forward. Published on March 27, 2008 as DOI: 10.1124/mol.108.045591
This article has not been copyedited and formatted. The final version may differ from this version.

gating kinetics and drug effects were based on a hERG gating model described previously (Wang *et al.,* 1997) using a computer program, ModelMaker4 (AP Benson Ltd).

6. **Drug solutions and application**

PD307243 and NS1643 were generous gift from Dr. Xiaoping Xu (GlaxoSmithKline). Their stock solutions (10 mM in DMSO) were divided into 100 ul aliquots, and stored at -20^{o}C until experiments. On the day of experiments, an aliquot was thawed, kept on ice and protected from light during the course of the experiments. In early experiments, we applied these drugs using the superfusion (flow-bath) method. The stock solutions were added to the low-[Cl] ND96 to reach desired final concentrations and the oocytes were superfused with the drug-containing solutions. In most of the experiments reported here, we applied the drugs using a 'non-flow' bath method. The oocytes were placed in 0.8 ml of low-[Cl] ND96 without superfusion, and impaled with two electrodes. After obtaining the control data, PD307243 or NS1643 stock solution was mixed with 0.2 ml low-[Cl] ND96 (to reach the desired final concentration when diluted 5 fold) and added to the bath. The solution was mixed by gently pipetting the bath solution up-and-down. When using the non-flow bath method, the agar salt bridges connecting the 3 M KCl/Ag/AgCl grounding electrodes to the bath solution were made in 2 mM [K] to avoid leakage of K^+ ions into the bath solution. There were no discernible differences in results from these two methods of drug application and the data were pooled.

Other drugs used in the experiments included: BeKm-1 (recombinant form, Alomone Lab, 200 uM stock in ND96 containing 0.5% BSA, diluted to 10 nM final concentration by adding 50 nl of the stock to 1 ml of bath solution containing 0.5% BSA; BSA served to prevent peptide from sticking to plastic surface), tetrapentylammonium Cl (Sigma-Aldrich, 1 M stock in

Molecular Pharmacology Fast Forward. Published on March 27, 2008 as DOI: 10.1124/mol.108.045591
This article has not been copyedited and formatted. The final version may differ from this version.

water, final concentration 50 uM) and dofetilide (a gift from Pfizer, 1 mM stock in water, pH 3, final concentration 0.5 uM).

In the experiments shown in Fig. 5, PD307243, NS1643 and TEA were injected into oocytes during the course of recording. The micro-dispenser injecting device was the same as that used for cRNA injection. Assuming an oocyte volume of 0.5 ul (sphere with 1 mm diameter), the following stock solutions and injection volumes were used to reach the estimated final cytoplasmic concentrations: PD307243 -15 nl of 10 mM stock to reach 300 uM, NS1643 - 20 nl of 25 mM stock to reach 1000 uM, and TEA - 20 nl of 50 mM stock to reach 2 mM.

7. **Chemical analysis of PD307243**

Because the effects of PD307243 on hERG reported here differed markedly from those reported previously (Gordon *et al*., 2008), we analyzed the chemical structure of PD307243 used in our experiments. ^{1}H-NMR and ^{13}C-NMR spectra were recorded at 300 MHz and at 75 MHz, respectively. Electronspray ionization (ESI) mass spectrum was performed on a Waters MZQ Micromass ZQ 4000. High resolution mass spectrum (HRMS) was recorded on a Thermo Finnigan Mat 95XP. Results are presented as *Supplemental Data*.

RESULTS

1. **PD307243 and NS1643 exerted 'activator' effects on the hERG channel and altered the channel's gating kinetics**

Figs. 1 and 2 illustrate detailed characterization of the effects of PD307243 and NS1643 (abbreviated as PD and NS in the following text) on the hERG channel expressed in oocytes. Both drugs increased the hERG current amplitude in a concentration-dependent manner (Figs.

Molecular Pharmacology Fast Forward. Published on March 27, 2008 as DOI: 10.1124/mol.108.045591
This article has not been copyedited and formatted. The final version may differ from this version.

1A and 2A). Such 'activator' effects were seen in both outward and inward currents (Figs. 1H and 2H). In most experiments, we used the test pulse current amplitude at 0 mV to quantify drugs' activator effects (except data in Figs. 5 - 7, noted in the figures or legends). We wished to compare the apparent binding affinity and potency of the activator effect between PD and NS. Assuming that both activators bound to the hERG channel in a 1:1 stoichiometry, and activator binding increased the current amplitude to 'A' fold of control, the drug-channel interaction could be described by the scheme.

At equilibrium in the presence of activator concentration [D], $R = K_d/([D] + K_d)$, $R^* = [D]/([D] + K_d)$. The ratio of current amplitude in the presence of activator (I_d) to control (I_c) will be: $I_d/I_c = R + (R^*A)$. This leads to equation [1] describing the relationship between I_d/I_c and [D]:

$$I_d/I_c = 1 + (A - 1)/(1 + K_d/[D]) \qquad [1]$$

Because PD had a secondary current-suppressing effect on the hERG channel (that became more apparent at concentrations $\geq$ 20 uM, or in the presence of pore blockers, see below), we fit the concentration-response relationship for [PD] 1 - 10 uM. The 'A' value was 2, and K_d value was 3 uM (Fig. 1B). In some oocytes NS at concentrations $\geq$ 60 uM induced a membrane 'leak' conductance (thus the large standard error bars at 60 and 90 uM in Fig. 2B). Nevertheless, we fit the complete concentration-response relationship of NS (3 - 90 uM) with equation [1], and obtained 'A' and K_d values of 3.24 and 20 uM, respectively. In the following experiments, we used [PD] of 10 or 20 uM and [NS] of 30 uM, i.e. concentrations that could induce significant effects on the hERG current amplitude without appreciable secondary current-suppressing or leak-inducing effects.

Both activators slowed the inactivation rate of the hERG channel to ~ 50% of control, without altering its voltage-sensitivity (Figs. 1G and 2G). However, the two differed in how they

Molecular Pharmacology Fast Forward. Published on March 27, 2008 as DOI: 10.1124/mol.108.045591
This article has not been copyedited and formatted. The final version may differ from this version.

influenced the activation/deactivation gating processes of the hERG channel. PD did not shift the voltage-dependence of activation (measured by the 1-s isochronal activation curve, Fig. 1C). It had no effect on the rate of hERG activation (measured by the 'envelope' voltage clamp protocol shown in Fig. 1E), or the time course of deactivation (quantified by double-exponential curve fitting, Fig. 1F). On the other hand, NS consistently shifted the 1-s isochronal activation curve in the negative direction (by ~ 10 mV) and accelerated hERG activation (Fig. 2C and 2E). NS also slowed the rate of hERG deactivation, manifested by a prolongation of the fast and slow time constants (Fig. 2F), although the distribution of the 2 components at different voltages was not affected (data not shown). PD and NS also differed in the voltage-dependence of their activator effects on the test pulse current (measured by current ratio or I_d/I_c). While the value of I_d/I_c for PD showed an increase with stronger depolarization (Fig. 1D), the opposite was seen with NS (Fig. 2D).

2. **Could the activator effects of PD307243 and NS1643 be accounted for by their effects on hERG channel gating kinetics?**

We used a kinetic model for hERG channel gating described previously (Wang *et al*., 1997) to test whether the activator effect of PD on the hERG channel could be accounted for by the drug-induced slowing of inactivation. The kinetic model and parameter values used in the simulations are described in Table 1. The only change we made for PD was a 50% decrease in the forward rate of channel inactivation, in accordance with the experimental data shown in Fig. 1: PD reduced the rate of hERG inactivation by 50% without changing its voltage-sensitivity, or parameter values related to the activation/deactivation gating processes. The simulation results are shown in Fig. 3A. The model could qualitatively mimic the effects of PD on hERG test pulse

Molecular Pharmacology Fast Forward. Published on March 27, 2008 as DOI: 10.1124/mol.108.045591
This article has not been copyedited and formatted. The final version may differ from this version.

currents (panels a and c), tail currents (a) and rate of inactivation (d). There was no shift in the voltage-dependence of activation (b).

To check whether we could simulate the NS effects on the hERG channel, we made the following changes in the model parameters: (1) forward rate constant of inactivation reduced by 50%, based on the slowing effect of NS on the rate of inactivation without altering the voltage-sensitivity, (2) forward rate constant from C_2 to O states increased to 4 fold, and (3) backward rate constant from O to C_2 decreased by 75%. We chose to modify the transition rates between the O state and the immediate C_2 state based on the experimental data shown in Fig. 2F. The time course of hERG channel deactivation could be described by a double exponential function in the V_r range > -100 mV, but mainly a single (fast) exponential function in more negative V_r range. The probable explanation for this kinetic behavior is that the fast deactivation component is mainly due to the backward transition from the O state to the immediate closed state, while the slow deactivation component is due to the residual forward transitions between closed states in the less negative voltage range. Therefore, to be consistent with the finding that NS significantly slowed the fast component of deactivation even at -120 mV, we altered the transition between O and C_2 states. The amount of changes described above was needed to reproduce the negative shift in the activation curve by -10 mV (Fig. 2C). The results of simulation of the NS effects are shown in Fig. 3B. The model qualitatively mimicked the effects of NS on the test pulse current (panels a and c), tail current (a), rate of inactivation (d) and voltage-dependence of activation (b).

Fig. 4 shows the concentration-response relationships of PD and NS on the hERG channel. The data support the above notion that PD's agonist effect was accompanied mainly by a slowing of hERG inactivation, while NS's agonist effect had contribution from both a slowing of hERG inactivation and a stabilization of the channel in the activated vs closed states (denoted

Molecular Pharmacology Fast Forward. Published on March 27, 2008 as DOI: 10.1124/mol.108.045591
This article has not been copyedited and formatted. The final version may differ from this version.

by the negative shift in $V_{0.5}$ of activation). Model prediction of the agonist effects of PD and NS appeared less than those observed experimentally (Figs. 1 and 2). Prolonged whole cell recording was accompanied by a gradual run-up of the hERG current amplitudes (Fig. S1 in *Supplemental Data*), that could cause an overestimation of the agonist effects.

The model-predicted relationship between 'V_t' and 'I_d/I_c' provided an explanation for the experimental findings of opposite trends for PD vs NS (Fig. 1D and 2D). For the PD simulation, the values of I_d/I_c gradually increased as the V_t became more depolarized, and plateaued at $V_t \geq$ +40 mV. This was due to the fact that the only change we introduced for PD in the hERG gating model was a reduction in the forward transition rate from O to I states, which was voltage-sensitive. As V_t became more depolarized, the rate of inactivation became a more dominating factor in determining the current amplitude, and thus slowing it would cause a higher % of increase in the current amplitude. For the NS simulation, the I_d/I_c value was highest at the threshold depolarization voltage, and steadily declined as V_t became more depolarized, approaching a steady level at $V_t \geq$ +20 mV. This was due to the fact that NS caused a more prominent increase in channel open probability at more negative V_t (but above the threshold of activation, panel b). This trend contributed to the higher I_d/I_c values from -60 to +20 mV. At more positive V_t, slowing of inactivation was the main factor for the increase in current amplitude, as in PD simulation, and I_d/I_c approached a similar value of ~2.

3. **Both PD307243 and NS1643 acted on the hERG channel from the extracellular side of the cell membrane but their effects were additive**

A prerequisite for the search of a drug's binding site in a membrane channel is to know whether there is 'membrane sidedness' in the drug's actions, i.e. whether the drug is effective only

Molecular Pharmacology Fast Forward. Published on March 27, 2008 as DOI: 10.1124/mol.108.045591
This article has not been copyedited and formatted. The final version may differ from this version.

when applied from inside or outside the cell membrane. Once this information is available, proper strategies can be designed (e.g. site-specific mutations, pharmacological or ionic perturbations) to gain further insights into the channel domain(s) where the drug may bind. Figs. 1A and 2A show that the effects of PD and NS (applied by directly adding the drug solution to the bath solution followed by pipetting up-and-down to mix the two, the 'non-flow' bath, see *Methods*) had very rapid onset, and the activator effects could be seen in the low uM concentration range. Importantly, the potency of PD tested in oocytes was not different from that of PD tested in mammalian COS-7 cells (Figs. 5A vs 5B). If these activators worked on the hERG channel from the intracellular side of the cell membrane, the yolk inside oocytes would provide a huge sink for the lipophilic drug molecules, leading to a decrease in the apparent drug potency and a delay in the onset of drug effects, as is the case for quinidine (Yeola *et al.*, 1996; Zhang *et al.*, 1998). Since COS-7 cells do not have yolk, we expected to see much higher drug potency when tested in the mammalian cells vs in oocytes. To check whether PD and NS worked on the hERG channel from the extracellular side of the cell membrane, we directly compared the potency of these drugs applied by intra-oocyte injection vs by bath application. Figs. 5B and 5C show that intra-oocyte injection of a high concentration of PD (300 uM) or NS (1000 uM) had no discernible effect on the hERG current amplitude or gating kinetics. However, subsequent bath application of a 30-fold lower concentration of PD (10 uM) or NS (30 uM) effectively increased the hERG current amplitude. To confirm the effectiveness of our intra-oocyte injection technique, in both experiments we pulled out the injecting pipettes, expelled the remaining drug solutions in the pipette tips, refilled the pipette tips with a TEA solution, reimpaled the oocytes and injected ~ 20 nl of TEA solution into the oocytes (comparable to the volume of drug solution injected). In both cases, intra-oocyte injection of TEA to reach an estimated cytoplasmic

Molecular Pharmacology Fast Forward. Published on March 27, 2008 as DOI: 10.1124/mol.108.045591
This article has not been copyedited and formatted. The final version may differ from this version.

concentration of 2 mM effectively suppressed the hERG current. These observations confirmed that both PD and NS worked on the hERG channel from the extracellular side of the cell membrane. The apparent slow onset of drug effects shown in Fig. 5A-C was due to the slow superfusion rate in these experiments to conserve drugs.

We further tested whether the effects of PD and NS were related to each other in binding site or mechanism of action. In these experiments, PD 20 uM was applied to the hERG channel expressed in oocytes using direct pipetting. After PD effect stabilized, NS 30 uM was applied in the continuous presence of PD. NS effects were compared with those measured in the absence of PD. Fig. 5D shows that NS was equally effective in increasing hERG current without or with PD, suggesting that the binding sites and mechanisms of action of these two hERG activators are independent of each other.

4. **Cys substitutions introduced into the outer vestibule or the external pore entrance of the hERG channel, or modifications of the engineered Cys side chains, differentially affected the activator actions of PD307243 and NS1643**

Since both PD and NS worked from the extracellular side of the cell membrane and both slowed the rate of hERG inactivation, our search for the drug binding sites targeted the outer vestibule region and the pore entrance. It has been proposed that the hERG channel's inactivation process is similar to the P-type inactivation described for the Shaker or Shaker-like channels (Fan *et al.*, 1999; Lopez-Barneo *et al.*, 1993; Smith *et al.*, 1996). The P-type inactivation is believed to arise from conformational changes around the outer mouth and in the pore-loop, that alter ion selectivity or conductance of the selectivity filter and shut down K^+ ion flux through the pore. Previously, we showed that the unusually long (~ 43 amino acids) extracellular S5-P linker

Molecular Pharmacology Fast Forward. Published on March 27, 2008 as DOI: 10.1124/mol.108.045591
This article has not been copyedited and formatted. The final version may differ from this version.

in the hERG channel also plays a critical role in the channel's inactivation process (Liu *et al*., 2002). Mutations introduced into specific 'high-impact' positions along the S5-P linker can disrupt the inactivation process (Dun *et al.*, 1999; Liu *et al*., 2002). The 4 S5- P linkers in a tetrameric hERG channel, along with the P-S6 linkers, line the outer vestibule of the channel. Since mutations along the S5-P linker that disrupted inactivation also impaired the hERG channel's ability to select for K^+ ions (Dun *et al*., 1999; Liu *et al*., 2002), the linker must interact with the pore loop in 3-D space. Indeed, our recent 3-D model for hERG's pore domain, based on peptide toxin foot-printing experiments and homology modeling, suggested that side chains at several 'high-impact' positions could make contact with pore-loop residues (Tseng *et al.*, 2007). We have performed a detailed Cys-scanning mutagenesis study of the S5-P linker in the hERG channel, and identified not only high-impact positions, but also 'intermediate-impact' positions (Liu *et al*., 2002). Cys substitution *per se* at the intermediate-impact positions does not disrupt the inactivation process or the pore's K^+ selectivity. However, modification of Cys side chains at these positions markedly impacted on channel function. Furthermore, our data suggested that the middle segment of the S5-P linker (positions 583 - 597) might adopt an α-helical structure. This was confirmed by subsequent experiments using NMR spectroscopy (Jiang *et al.*, 2005; Torres *et al*., 2003). Interestingly, Cys side chains engineered into most positions along this 'S5-P helix' could form intersubunit disulfide bonds (Jiang *et al*., 2005). We further showed that Cys side chain introduced into position 584, 585, 588, and 589 on the S5-P helix could form intersubunit disulfide bond with counterparts from adjacent subunits (Jiang *et al*., 2005). This may also be the case for Cys side chain introduced into position 631 at the external pore entrance. In all cases, disulfide bond formation disrupted the inactivation process and the K^+ selectivity.

Molecular Pharmacology Fast Forward. Published on March 27, 2008 as DOI: 10.1124/mol.108.045591
This article has not been copyedited and formatted. The final version may differ from this version.

We took advantage of the available information and mutant channels to address the following question: how do Cys side chains introduced into the S5-P linker and the pore entrance positions, or a modification of these engineered Cys side chains, impact on the activator effects of PD and NS? We selected eight Cys substituted mutants that covered the region of interest (diagrammed in Fig. 6A). In all cases, oocytes were treated with DTT to reduce spontaneously formed disulfide bonds. In cases when disulfide bonds were needed to create the mutant phenotype (G584C, H587C and S631C), oocytes were treated with H_2O_2 (0.3%) in conjunction with depolarizing pulses (or incubated in elevated $[K]_o$ 20 mM) to facilitate intersubunit disulfide bond formation. The mutant phenotype was identified by a lack of bell-shaped current-voltage relationships (as shown in Fig. 1D and 1H), due to a disruption of the inactivation process. Furthermore, tail currents recorded at -60 or -80 mV turned in the inward direction, due to a loss of K^+ selectivity (so that extracellular Na^+ ions carried inward tail currents at these voltages). To guard against artifacts due to interference from oocyte endogenous currents, we confirmed that (1) currents in DTT-treated oocytes that had been injected with cRNAs for the Cys-substituted mutants were significantly larger than currents in uninjected oocytes, and (2) PD at 20 uM had no noticeable effects on currents in uninjected oocytes (data not shown).

We quantified drug effects on current amplitudes through channels with the mutant phenotype from test pulse currents measured at +60 mV, the highest amounts of outward current in the voltage range tested. PD 20 uM or NS 30 uM was applied to the bath solution by direct pipetting. Drug effects were evaluated in a 'yes-or-no' fashion. We did not attempt to quantitatively compare the degrees of drugs' activator effects among the channels. Fig. 6B shows that PD was effective in increasing currents through all the channels in either the WT-like or the mutant mode. Therefore, conformational changes in the outer vestibule or the pore entrance did

Molecular Pharmacology Fast Forward. Published on March 27, 2008 as DOI: 10.1124/mol.108.045591
This article has not been copyedited and formatted. The final version may differ from this version.

not prevent the activator effect of PD. This is the case even with intersubunit disulfide bond formation in G584C, H587C or S631C, which was expected to alter the peptide backbone conformation and flexibility. On the other hand, although NS was effective in increasing currents through the channels when they were in the WT-like gating mode, the drug could not induce the activator effect when the channels were in the mutant mode (Fig. 6C).

Original data are shown in Figs. 6D and Fig. 7 to support the above conclusions. Fig. 6D illustrates representative current traces recorded from G572C, G584C (disulfide bonded), W585C, H587C (disulfide bonded), and N588C. NS 30 uM did not induce the activator effect (and a modest current-suppressing effect on W585C was revealed). In the continuous presence of NS, PD 20 uM effectively increased outward current at +60 mV as well as inward current at -120 mV. Fig. 7 illustrates the impact of modifying Cys side chains introduced into the external pore entrance, T613C and S631C. Cys substitution *per se* (in the free thiol state) at these 2 positions did not affect the channel function: they were WT-like in showing strong inactivation and K^+ selectivity. However, MTSET modification of T613C impaired the channel's ability to inactivate or to select for K^+ ions (Fig. 7A). Treating S631C with 0.3% H_2O_2 while depolarizing the membrane to cause channel activation and inactivation effectively converted the S631C channel to the mutant phenotype: impaired inactivation and K^+ selectivity (Fig. 7B) (Fan *et al*., 1999). PD 20 uM effectively increased both outward currents and inward currents through the T613C and S631C channels in both WT-like and mutant modes (left columns of Figs. 7C and 7D). On the other hand, although NS 30 uM was effective in increasing currents through the two channels when they were in the WT-like mode, it could not induce any activator effect when the channels were in the mutant mode (right columns of Figs. 7C and 7D). Note that MTEST, DTT or H_2O_2

Molecular Pharmacology Fast Forward. Published on March 27, 2008 as DOI: 10.1124/mol.108.045591
This article has not been copyedited and formatted. The final version may differ from this version.

had no effect on the gating kinetics or K^+ selectivity of WT hERG (Fan *et al*., 1999). DTT or H_2O_2 treatment did not impair the agonist effect of NS on WT hERG (data not shown).

5. **Using external and internal hERG pore blockers to further probe the sites for the activator actions of PD307243 and NS1643**

Previously, we showed that a scorpion peptide toxin, BeKm-1, binds to the outer vestibule of the hERG channel to suppress its currents (Fig. 8A) (Zhang *et al*., 2003). We further identified the following hERG residues that are likely to make direct contacts with the bound BeKm-1 peptide: R582, I583, Y597 (at the two ends of the S5-P helix) and S631 (at the pore entrance) (Tseng *et al*., 2007). We hypothesized that BeKm-1 binding might differentially impact on the binding and/or action of PD and NS. Indeed, Figs. 8B - 8D show that BeKm-1 potentiated PD's activator effect while suppressed NS's activator effect.

Positively charged quaternary ammonium cations (QA^+) have been used as a tool to probe the ion conduction pathway of K channels (Ahern *et al.*, 2006). In the Shaker or Shaker-like channels, QA^+ applied from outside the cell membrane binds to the external pore entrance to occlude currents through the pore. Although extracellular TEA has a low binding affinity to hERG (50% reduction at ~ 50 mM) (Pardo-Lopez *et al.*, 2002), lengthening the hydrocarbon chain length greatly increased the binding affinity, so that 50 uM tetrapentyl ammonium cation ($TPeA^+$) could suppress the current by $\geq$ 80% (Fig. 9A). $TPeA^+$ effectively prevented the activator effect of PD. Instead, $TPeA^+$ unmasked a concentration-dependent current suppressing effect of PD (Fig. 9B).

Dofetilide binds to the hERG channel from the intracellular side of the cell membrane (Kamiya *et al*., 2006). An Ala scanning mutagenesis approach has been used to probe the

Molecular Pharmacology Fast Forward. Published on March 27, 2008 as DOI: 10.1124/mol.108.045591
This article has not been copyedited and formatted. The final version may differ from this version.

dofetilide binding site in the hERG channel (Kamiya *et al*., 2006): Y652A, F656A on the S6 helix, T623A, S624A and V625A along the selectivity filter of the pore-loop, as well as G648 (on S6, juxtaposed to the pore-loop) greatly attenuated the dofetilide binding affinity. Therefore the dofetilide binding site is likely formed with S6 helices and roofed by the pore-loop (cartoon in Fig. 9C). Applying dofetilide 0.5 uM to hERG expressed in oocytes in conjunction with constant pulsing to cause channel activation led to a gradual decrease in current amplitude, reaching a suppression of $\geq$ 80% in 15-20 min (Fig. 9D). Under these conditions, dofetilide effectively prevented the activator effect of PD, and unmasked its current suppressing effect. Thus, although the PD's activator effect on the hERG channel could not be disrupted by interventions applied to the extracellular S5-P linker or the external pore entrance, it was prevented by blockers that could reduce K^+ ion occupancy in the selectivity filter of the hERG channel (more in *Discussion*).

DISCUSSION

The major findings in this study can be summarized as the following. The concentration-response relationships of PD and NS on the hERG channel could be described by a 1:1 binding stoichiometry, with the maximal effect being 100% and $\geq$ 300% increase in the current amplitude (measured as time-dependent current during 1-s step to 0 mV) with apparent K_d values of 3 and 20 uM, respectively. The activator effect of PD was accompanied by a slowing of hERG inactivation. On the other hand, the activator effect of NS involved not only a slowing of hERG inactivation, but also an acceleration of channel activation as well as retardation of channel deactivation. Both drugs worked on the hERG channel from the extracellular side of the cell membrane. Inactivation-disrupting mutations or side chain modifications introduced into the

Molecular Pharmacology Fast Forward. Published on March 27, 2008 as DOI: 10.1124/mol.108.045591
This article has not been copyedited and formatted. The final version may differ from this version.

outer vestibule or pore entrance of the hERG channel abolished the activator effect of NS, but did not prevent the activator effect of PD. BeKm-1, a peptide toxin that bound to the outer vestibule of the hERG channel (Tseng *et al*., 2007) greatly attenuated the activator effect of NS, but potentiated the activator effect of PD. Finally, the activator effect of PD was prevented by an external pore blocker, tetrapentylammonium (Ahern *et al*., 2006), or by dofetilide that is known to bind to the inner cavity of the hERG channel (Kamiya *et al*., 2006).

1. Binding site and mechanism of action of NS1643

Our data support the notion that the NS binding site is formed by the outer vestibule and pore entrance of the hERG channel. The positions where Cys substitution or side chain modification abolished NS's activator effects (e.g. 572 at the extracellular end of S5, positions along the S5-P helix between 584 and 593, 613 and 631 at the external pore entrance) may be close to each other in 3-D space (Fig. S2 in *Supplemental Data*). Our previous studies suggested that the S5-P helices in the hERG channel must be able to adopt dynamic conformational changes during membrane depolarization, so that a considerable portion of their surfaces can come close to each other to allow intersubunit disulfide bond formation between Cys side chains at equivalent positions (Jiang *et al*., 2005). Furthermore, our 3-D model of the hERG channel pore domain suggested that W585 and L589 side chains on the S5-P helices can make contacts with pore-loop side chains (Tseng *et al*., 2007), providing an explanation for why mutations along the S5-P linker can impact on the channel's K^+ selectivity (Tseng *et al*., 2007).

It is not surprising that putative NS binding to a domain formed by the outer vestibule/external pore entrance can influence the rates of activation and deactivation. These gating processes are believed to occur at the cytoplasmic halves of the S6 segments, controlled

Molecular Pharmacology Fast Forward. Published on March 27, 2008 as DOI: 10.1124/mol.108.045591
This article has not been copyedited and formatted. The final version may differ from this version.

by the voltage-sensor S4 via the S4-S5 linkers (Long *et al*., 2005). The extracellular end of S4 in the activated state can come close to the extracellular end of S5 from an adjacent subunit (to allow intersubunit disulfide bond formation) (Gandhi *et al.*, 2003; Laine *et al.*, 2003). Therefore, drug binding to the outer vestibule/external pore entrance may allosterically affect the stability of S4 segment in the activated state. Indeed, we have shown that Cys substitutions at high-impact positions in the outer vestibule of the hERG channel could affect not only inactivation/K^+ selectivity, but also the voltage-dependence of activation (Liu *et al*., 2002).

Our data are subject to alternative explanations. Data in Figs. 5 and 6 can be alternatively explained by a removal of the mechanism for NS action. Data in Fig. 8 can be alternatively explained by a reorientation of the channel upon BeKm-1 binding, preventing access to an NS binding site in other area(s) of the channel.

2. **Binding site and mechanism of action of PD307243**

The activator effect of PD was very robust. PD remained effective even when intersubunit disulfide bonds were formed between S5-P helices. Such intersubunit disulfide bonds were expected to perturb the peptide backbone conformation and flexibility. However, extracellularly applied TPeA and intracellularly-acting dofetilide prevented the activator effect of PD. What are the common features shared by these two pore blockers that acted from the opposite sides of the cell membrane? An X-crystallographic study has revealed the binding sites for external TEA and internal tetrabutylammonium (TBA) and their effects on Tl^+ (a K^+ analog) ion occupancy in the selectivity filter of the KscA channel (Lenaeus *et al.*, 2004). It is reasonable to apply information learned from the crystallographic work on KcsA to our study for the following reasons. First, it has been shown that the binding site and likely the mechanism of

Molecular Pharmacology Fast Forward. Published on March 27, 2008 as DOI: 10.1124/mol.108.045591
This article has not been copyedited and formatted. The final version may differ from this version.

action of extracellular quaternary ammonium (QA^+) cation are similar among different K channels (Ahern *et al*., 2006). Second, although TBA and dofetilide are distinctly different molecules, TBA binding to the KcsA channel and dofetilide binding to the hERG channel share two important features: (1) they both bind deep in the channel inner cavity, right beneath and likely making contact with the pore-loop, and (2) binding is stabilized by hydrophobic interactions between the blockers and aromatic residues facing toward the inner cavity (F103 in KcsA and the equivalent Y652 in hERG) (Kamiya *et al*., 2006; Lenaeus *et al*., 2004). External TEA binding and internal TBA binding to the KcsA channel share two features: (1) the selectivity filter becomes largely devoid of Tl^+ ions, and (2) the peptide backbone of the selectivity filter exhibits subtle conformational changes (Lenaeus *et al*., 2004). While these observations explain why external TEA and internal TBA (or external TPeA and internal dofetilide, in the case of hERG) can totally occlude K^+ ion flux through the pore, they also suggest that PD may be a 'pore modifier'.

To explain why PD is sensitive to the degree of K^+ ion occupancy in the selectivity filter, we hypothesize that PD directly acts on the pore-loop to increase channel conductance and secondarily/additionally retard hERG inactivation. Although we were able to qualitatively simulate PD effects on the WT hERG channel by a 50% reduction in the inactivation rate, introducing an increase in channel conductance in the parameter set might improve model simulation quantitatively. Interventions that disrupted hERG inactivation did not prevent PD's agonist effect. In these cases, PD might work by primarily increasing channel conductance, although the interventions might have also affected PD binding affinity and/or degree of increase in the channel conductance. To provide direct experimental evidence for the hypothesis, we need to perform outside-out patch recordings of single channel currents through WT and inactivation-

Molecular Pharmacology Fast Forward. Published on March 27, 2008 as DOI: 10.1124/mol.108.045591
This article has not been copyedited and formatted. The final version may differ from this version.

disrupted channels under the control conditions and after the application of increasing concentrations of PD. Such extensive experiments are beyond the scope of the current study.

BeKm-1 potentiated the activator effect of PD. What are the differences between TPeA and BeKm-1, both of which bound to the outer mouth of the hERG channel? BeKm-1 differs from TPeA in two aspects. First, the peptide toxin binds above the pore entrance, and does not totally occlude K^+ ion flux through the pore (Tseng *et al*., 2007; Zhang *et al*., 2003). Second, BeKm-1 binds to the hERG outer vestibule in the resting and activated states but unbinds in the inactivated state, probably due to the dynamic conformational changes in this region discussed above (Tseng *et al*., 2007). Therefore, the extracellular BeKm-1 peptides may go through binding and unbinding cycles under our voltage clamp conditions, and the presence of PD through its pore-modifier effect may retard BeKm-1 binding or facilitate BeKm-1 unbinding, producing an apparent potentiation of its activator effect.

3. Comparison with previous studies

Our results on NS1643 are consistent with a previous study (Casis *et al*., 2006): pore mutations that impair hERG inactivation (S631A, G628C/S631C and S620T) attenuate the activator effect of NS. Our results on PD307243 are similar to a previous study on its structure analog, PD118057 (Zhou *et al*., 2005): PD118057 did not affect the voltage-dependence or kinetics of activation and deactivation, and it slowed the rate of hERG inactivation at 35^{o}C. A recent report on PD307243 (1 - 10 uM, applied to the hERG channel stably expressed in CHO cells) had some very novel findings (Gordon *et al*., 2008). The authors showed that PD307243 not only increased the hERG current amplitude, but also created a prominent constitutive component and greatly slowed the rate of channel inactivation. The combined effects of

Molecular Pharmacology Fast Forward. Published on March 27, 2008 as DOI: 10.1124/mol.108.045591
This article has not been copyedited and formatted. The final version may differ from this version.

constitutive channel activation and markedly slowed inactivation created a peculiar transient outward (I_{to})-like current. We have not observed such a PD-induced I_{to}-like current or constitutive channel activation in oocytes or COS-7 cells. We have confirmed the chemical structure of PD307243 used in our experiments (*Supplemental Data*). Importantly, we have confirmed the agonist effect of PD on native I_{Kr} in guinea pig ventricular myocytes (Fig. 10). In 3 separate experiments, 10 uM PD increased the time-dependent outward current recorded at -10 or -20 mV (mainly reflecting I_{Kr}) by 41, 95 and 193% after exposure times of 1.5, 4 and 7 min, respectively. PD did not induce any I_{to}-like current in guinea pig ventricular myocytes.

ACKNOWLEDGEMENTS

We would like to thank Dr. Xiaoping Xu, Cardiovascular and Urogenital Center of Excellence in Drug Discovery, GlaxoSmithKline, for providing PD307243 and NS1643.

Molecular Pharmacology Fast Forward. Published on March 27, 2008 as DOI: 10.1124/mol.108.045591
This article has not been copyedited and formatted. The final version may differ from this version.

REFERENCES

Ahern CA, Eastwood AL, Lester HA, Dougherty DA, and Horn R. (2006) A cation-π interaction between extracellular TEA and an aromatic residue in potassium channels. J Gen Physiol **128**:649-657.

Brugada R, Hong K, Dumaine R, Cordeiro JM, Gaita F, Borggrefe M, Menendez TM, Brugada J, Pollevick GD, Wolpert C, Burashnikov E, Matsuo K, Wu YS, Guerchicoff A, Bianchi F, Giustetto C, Schimpf R, Brugada P, and Antzelevitch C. (2004) Sudden death associated with short-QT syndrome linked to mutations in HERG. Circulation **109**:30-35.

Casis O, Olesen S-P, and Sanguinetti MC. (2006) Mechanism of action of a novel human ether-a-go-go-related gene channel activator. Mol Pharm **69**:658-665.

Dun W, Jiang M, and Tseng G-N. (1999) Allosteric effects of mutations in the extracellular S5-P loop on the gating and ion permeation properties of *hERG*. Pflugers Archiv **439**:141-149.

Fan J-S, Jiang M, Dun W, McDonald TV, and Tseng G-N. (1999) Effects of outer mouth mutations on *hERG* channel function: a comparison with similar mutations in *Shaker*. Biophys J **76**:3128-3140.

Gandhi CS, Clark E, Loots E, Pralle A, and Isacoff EY. (2003) The orientation and molecular movement of a K^+ channel voltage-sensing domain. Neuron **40**:515-525.

Gordon E, Lozinskaya IM, Lin Z, Seus SF, Blaney FE, Willette RN, and Xu X. (2008) 2-[2-(3,4-dichloro-phenyl)-2,3-dihydro-1H-isoindol-5-ylamino]-nicotinic acid (PD-307243) causes instantaneous current through human ether-a-go-go-related gene potassium channels. Mol Pharm 73;639-651.

Hansen RS, Diness TG, Christ T, Demnitz J, Ravens U, Olesen S-P, and Grunnet M. (2006) Activation of human ether-a-go-go-related gene potassium channels by the diphenylurea 1,3-bis-(2-hydroxy-5-trifluoromethy-phenyl)-urea (NS1643). Mol Pharm **69**:266-277.

Jiang M, Zhang M, Maslennikov IV, Liu J, Wu DM, Korolkova YV, Arseniev AS, Grishin EV, and Tseng G-N. (2005) Dynamic conformational changes of extracellular S5-P linkers in the hERG channel. J Physiol **569**:75-89.

Kamiya K, Niwa R, Mitcheson JS, and Sanguinetti MC. (2006) Molecular determinants of hERG channel block. Mol Pharm **69**:1709-1716.

Kang J, Chen X-L, Wang H, Ji J, Cheng H, Incardona J, Reynolds W, Viviani F, Tabart M, and Rampe D. (2005) Discovery of a small molecule activator of the human ether-a-go-go-related gene (HERG) cardiac K^+ channel. Mol Pharm **67**:827-836.

Laine M, Lin M-CA, Bannister JPA, Silverman WR, Mock AF, Roux B, and Papazian DM. (2003) Atomic proximity between S4 segment and pore domain in Shaker potassium channels. Neuron **39**:467-481.

Lenaeus MJ, Vamvouka M, Focia PJ, and Gross A. (2004) Structural basis of TEA blockade in a model potassium channel. Nature Structural & Molecular Biology **12**:454-459.

Liu J, Zhang M, Jiang M, and Tseng G-N. (2002) Structural and functional role of the extracellular S5-P linker in the HERG potassium channel. J Gen Physiol **120**:723-737.

Long SB, Campbell EB, and MacKinnon R. (2005) Voltage sensor of Kv1.2: structural basis of electromechanical coupling. Science **309**:903-908.

Lopez-Barneo J, Hoshi T, Heinemann SH, and Aldrich RW. (1993) Effects of external cations and mutations in the pore region on C-type inactivation of Shaker potassium channels. Receptors and channels **1**:61-71.

Pardo-Lopez L, Zhang M, Liu J, Jiang M, Possani LD, and Tseng G-N. (2002) Mapping the binding site of a HERG-specific peptide toxin (ErgTx) to the channel's outer vestibule. J Biol Chem **277**:16403-16411.

Perry M, Saches FB, and Sanguinetti MC. (2007) Structural basis of action of a human ether-a-go-go-related gene 1 potassium channel activator. PNAS **104**:13827-13832.

Recanatini M, Poluzzi E, Masetti M, Cavalli A, and De Ponti F. (2005) QT prolongation through hERG K^+ channel blockade: current knowledge and strategies for the early prediction during drug development. Med Res Rev **25**:133-166.

Roden DM. (2004) Drug-induced prolongation of the QT interval. New England Journal of Medicine **350**:1013-1022.

Sanguinetti MC, Jiang C, Curran ME, and Keating MT. (1995) A mechanistic link between an inherited and an acquired cardiac arrhythmia: HERG encodes the I_{Kr} potassium channel. Cell, **81**:299-307.

Sanguinetti MC and Jurkiewicz NK. (1990) Two components of cardiac delayed rectifier K^+ current. Differential sensitivity to block by class III antiarrhythmic agents. J Gen Physiol **96**:195-215.

Schreibmayer W, Lester HA, and Dascal N. (1994) Voltage clamping of Xenopus laevis oocytes utilizing agarose-cushion electrodes. Pflugers Archiv **426**:453-458.

Smith PL, Baukrowitz T, and Yellen G. (1996) The inward rectification mechanism of the HERG cardiac potassium channel. Nature **379**:833-836.

Torres AM, Bansal P, Sunde M, Clarke CE, Bursill JA, Smith DJ, Bauskin A, Breit SN, Campbell TJ, Alewood PF, Kuchel PW, and Vandenberg JI. (2003) Structure of the HERG K^+ channel S5P extracellular linker: role of an amphipathic α-helix in C-type inactivation. J Biol Chem **278**:42136-42148.

Tseng G-N. (2001) I_{Kr}: the hERG channel. J Mol Cell Cardiol **33**:835-849.

Tseng G-N, Sonawane KD, Korolkova YV, Zhang M, Liu J, Grishin E, and Guy HR. (2007) Probing outer mouth structure of the hERG channel with peptide toxin foot printing and molecular modeling. Biophys J **92**:3524-3540.

Wang S, Liu S, Morales MJ, Strauss HC, and Rasmusson RL. (1997) A quantitative analysis of the activation and inactivation kinetics of *HERG* expressed in *Xenopus* oocytes. J Physiol **502**:45-60.

Yao J-A, Jiang M, Fan J-S, Zhou Y-Y, and Tseng G-N. (1999) Heterogeneous changes in K currents in rat ventricles three days after myocardial infarction. Cardiov Res **44**:132-145.

Yeola SW, Rich TC, Uebele VN, Tamkun MM, and Snyders DJ. (1996) Molecular analysis of a binding site for quinidine in a human cardiac delayed rectifier K^+ channel. Role of S6 in antiarrhythmic drug binding. Circ Res **78**:1105-1114.

Zhang H, Zhu B, Yao J-A, and Tseng G-N. (1998) Differential effects of S6 mutations on binding of quinidine and 4-aminopyridine to rKv1.4: common site but different factors in determining blockers' binding affinity. J Pharm Exp Ther **287**:332-343.

Zhang M, Korolkova YV, Liu J, Jiang M, Grishin EV, and Tseng G-N. (2003) BeKm-1 is a hERG-specific toxin that shares the structure with ChTx but the mechanism of action with ErgTx1. Biophys J **84**:3022-3036.

Zhou J, Augelli-Szafran CE, Bradley JA, Chen X, Koci BJ, Volberg WA, Sun Z, and Cordes JS. (2005) Novel potent human ether-a-go-go-related gene (hERG) potassium channel enhancers and their in vitro antiarrhythmic activity. Mol Pharm **68**:876-884.

Molecular Pharmacology Fast Forward. Published on March 27, 2008 as DOI: 10.1124/mol.108.045591
This article has not been copyedited and formatted. The final version may differ from this version.

Footnote to the title:

This study was supported by RO1 HL46451 and HL67840 (GNT) from the National Heart, Lung and Blood Institute of National Institutes of Health.

Molecular Pharmacology Fast Forward. Published on March 27, 2008 as DOI: 10.1124/mol.108.045591
This article has not been copyedited and formatted. The final version may differ from this version.

LEGENDS FOR FIGURES

Scheme legend: R and R* represent fractions of channels in activator-free and activator-bound states, D is activator drug, K_{on} and K_{off} are binding and unbinding rate constants, and K_d is dissociation constant.

Fig. 1 Characterization of the effects of PD 307243 (PD) on the hERG channel expressed in oocytes. (A) *Upper*: Superimposed hERG current traces before (black) and after PD application (1, 2, 5, 10, 20, and 50 uM, traces shown in the same colors as those of symbols in the lower panel). The currents were elicited by the voltage clamp protocol diagrammed on top applied once every min. *Lower*: Time course of changes in hERG current amplitude from the same experiment. Current amplitudes were measured from the time-dependent current during the 0 mV step and normalized by the control current right before the start of PD application. **(B)** Concentration-response relationship. Numbers of measurements are shown in parentheses. The superimposed curve was calculated from equation [1] (see text), with 'fold increase in current amplitude' (parameter 'A' in equation [1]) = 2, and apparent dissociation constant K_d = 3 uM. In the following panels, data points and current traces recorded under the control conditions are shown in black, and those recorded in the presence of PD (10 uM) are shown in red. **(C)** PD did not shift the 1-s isochronal activation curve of hERG. *Inset*: voltage clamp protocol and representative current traces. The relationship between V_t and peak amplitude of tail current (I_{tail}) was fit with a Boltzmann function: $I_{tail} = I_{max}/[1+\exp(V_{0.5}-V_t)/k]$, to estimate the maximal peak tail current amplitude (I_{max}), half-maximal activation voltage ($V_{0.5}$) and slope factor (k). I_{tail} was normalized by I_{max} (I_{tail}/I_{max} = fraction activated) and plotted against V_t. **(D)** PD increased hERG test pulse currents in a voltage-dependent manner. The voltage clamp protocol was the same as that described for panel (C). For each oocyte, amplitudes of time-dependent currents during 1-s

Molecular Pharmacology Fast Forward. Published on March 27, 2008 as DOI: 10.1124/mol.108.045591
This article has not been copyedited and formatted. The final version may differ from this version.

test pulses to V_t were normalized by the control current at V_t -10 mV. The current ratios, I_d/I_c, are also plotted based on the right coordinate. **(E)** PD did not alter the time course of hERG activation. *Inset*: 'envelope' voltage clamp protocol and representative current traces. The rate of hERG activation was slower than inactivation. Thus the time course of activation could not be directly measured from the test pulse currents. Since the outward tail currents signified channels recovered from inactivation, the time course of growth of peak tail current amplitude after increasing durations of depolarizing pulses could be used to infer the time course of channel activation. The membrane voltage was stepped to V_t for durations varying from 5 to 1000 ms in 50 ms increments. The time course of growth of peak tail current amplitude was fit with a single exponential function to generate $\tau_{activation}$ (plotted on a logarithmic scale so that the slope indicates the voltage-sensitivity of the underlying gating process). **(F)** PD did not alter the time course of hERG deactivation. *Inset*: voltage clamp protocol. Tail currents during 2- to 5-s step to V_r were fit with a double exponential function to generate the fast and slow time constants of deactivation (τ_{fast} and τ_{slow}, right and left coordinates, respectively). In V_r range $\leq$ -100 mV, channel deactivation was almost exclusively the fast component; thus τ_{slow} values are not shown. **(G)** PD modestly slowed the rate of hERG inactivation. *Inset*: triple-pulse voltage clamp protocol and representative current traces during the third step (indicated by gray shade in the protocol diagram). The blue trace represents control current trace scaled to match the amplitude of current in PD. hERG inactivation was faster than activation. To bypass the slow activation process, the hERG channels were first fully activated and inactivated by a 1-s step to +60 mV. This was followed by a brief 15-ms step to -80 mV during which the channels recovered from inactivation without appreciable deactivation. The third depolarizing step to various V_t caused channel transition from open to inactivated states. The decay of current traces during the third pulse was

Molecular Pharmacology Fast Forward. Published on March 27, 2008 as DOI: 10.1124/mol.108.045591
This article has not been copyedited and formatted. The final version may differ from this version.

fit with a single exponential function to generate time constant of inactivation ($\tau_{inactivation}$). The rate of inactivation (reciprocal of $\tau_{inactivation}$, left coordinate, logarithmic scale) was plotted against V_t. The relationship between the rate of inactivation and V_t in the range of 0 to +60 mV was fit with equation [2]: $K(V_t) = K(0)\exp(z_{ina}V_tF/RT)$, where $K(V_t)$ and $K(0)$ are rates of inactivation at V_t and 0 mV, respectively, z_{ina} is equivalent gating charge of inactivation, F, R and T are Faraday constant, gas constant and absolute temperature, respectively. The lines superimposed on the data points were calculated from equation [2], with $K(0)$ and z_{ina} values of 0.23 ms^{-1} and 0.72 for control, 0.12 ms^{-1} and 0.71 for PD. * $p < 0.05$, PD vs control. **(H)** PD increased both outward and inward currents through the hERG channel. The voltage clamp protocol was the same as that diagrammed in (F). For each cell, current amplitudes were measured from the peak or plateau level of tail currents (defined as fully-activated current, or I_{f-a}) and normalized by the control I_{f-a} at -50 mV.

Fig. 2 Characterization of the effects of NS 1643 (NS) on the hERG channel expressed in oocytes. Voltage clamp protocols and methods of data analysis are the same as those described for corresponding panels in Fig. 1. [NS] for experiments shown in panels (C)-(H) was 30 uM. **(A)** Time course of changes in hERG current amplitude before and during exposure to NS at the specified concentrations. **(B)** Concentration-response relationship. The superimposed curve was calculated from equation [1] with 'fold increase in current amplitude' = 3.24, K_d = 20 uM.**(C)** NS shifted the 1-s isochronal activation curve of hERG in the negative direction by -9.8$\pm$1.4 mV (n = 7). **(D)** NS increased hERG test pulse current in a voltage-dependent manner. **(E)** NS accelerated hERG activation (shortened $\tau_{activation}$). **(F)** NS slowed hERG deactivation, manifested as a prolongation of τ_{fast} and τ_{slow}. **(G)** NS slowed hERG inactivation. The lines superimposed on

Molecular Pharmacology Fast Forward. Published on March 27, 2008 as DOI: 10.1124/mol.108.045591
This article has not been copyedited and formatted. The final version may differ from this version.

the data points were calculated from equation [2] (described for Fig. 1G), with values of K(0) and z_{ina} 0.02 ms^{-1} and 0.6 for control, 0.01 ms^{-1} and 0.5 for PD. **(H)** NS increased both outward and inward currents through the hERG channel. * $p < 0.05$, NS vs control.

Fig. 3 Model simulation of the effects of PD307243 (A) and NS1643 (B) on the hERG channel. The model and parameter values are listed in Table1. Simulated current traces and data points for control, PD and NS are shown in black, red and blue, respectively. For each column, 'a' and 'd' show superimposed simulated current traces elicited by the voltage clamp protocols diagrammed in the insets (time scale was the same as protocols shown in Fig. 1), 'b' depicts simulated 1-s isochronal activation curves, and 'c' illustrates simulated test pulse current-voltage relationship (open symbols, left coordinate) and current ratio (I_d/I_c, right coordinate). Inset of panel Aa shows horizontally shifted inward tail currents at -120 mV, to illustrate the difference in the peak current amplitude.

Fig. 4 Concentration-response relationships of PD307243 (A) and NS1643 (B) on hERG current amplitude and gating kinetics. ΔAMP: % increase in current amplitude measured as time-dependent current during 1-s step to 0 mV. $\Delta V_{0.5}$: shift in $V_{0.5}$ of activation. $\Delta Rate_{INAC}$: % decrease in rate of channel inactivation at 0 mV. Data were averaged from 4 - 6 measurements each.

Fig. 5 Both PD307243 and NS1643 worked from outside the cell membrane yet their effects were independent of each other. (A) *Left*: Time course of changes in hERG current amplitude expressed in a COS-7 cell before, during, and after bath application of PD (PD_o, 10 uM), and

Molecular Pharmacology Fast Forward. Published on March 27, 2008 as DOI: 10.1124/mol.108.045591
This article has not been copyedited and formatted. The final version may differ from this version.

total current suppression by dofetilide (DOF). Currents were elicited by the voltage clamp protocol diagrammed on top of the right panel. Current amplitudes were measured from the peak of tail current at -60 mV and normalized by the control right before PD application. The time course of onset of PD effect was fit with a single exponential function with τ value of 6 min. *Right*: superimposed current traces from the same experiment at time points 'a', 'b' and 'c'. **(B)** and **(C)** *Left*: Time courses of changes in hERG current amplitude expressed in oocytes before and after intra-oocyte drug injection (estimated cytoplasmic concentrations denoted: PD_i ~ 300 uM and NS_i ~ 1000 uM), during exposure to drugs applied to the bath solution (PD_o 10 uM, NS_o 30 uM) and after intra-oocyte injection of TEA (TEA_i ~ 2 mM). In each experiment, the same injecting pipette was used first for PD or NS injection and then for TEA injection. *Right*: Superimposed current traces from the same experiments as in left panels at the specified time points. *Inset* of right panel in (B): % increase in hERG current amplitude caused by 10 uM PD tested in COS-7 cells and in oocytes measured from the peak amplitudes of outward tail currents at -60 mV (66$\pm$10 and 61$\pm$ 8, n = 4 and 20, $p > 0.05$). The same conclusion could be reached by measuring time-dependent test pulse currents at +40 mV: PD increased the current by 187$\pm$67% and 185$\pm$16% in COS-7 cells and in oocytes, respectively. **(D)** *Left*: Time course of changes in hERG current amplitude before and during bath application of 20 uM PD and after adding NS 30 uM in the continuous presence of PD. *Right*: % increase in current amplitude caused by NS in the absence or presence of PD ('-' and '+' PD).

Fig. 6 Summary of effects of Cys substitution or Cys side chain modification introduced into the outer vestibule or pore entrance of the hERG channel on the activator action of PD307243 and NS1643. (A) *Top*: 2-D diagram of a hERG subunit, marking S1 - S6

transmembrane helices, pore-loop, and the extracellular S5-P helix. *Lower*: amino acid sequence of the S5-P linker, marking the positions that participate in forming the S5-P helix. High- and intermediate-impact positions are highlighted by white letterings on black shade and by gray shade, respectively. The positions examined in Figs. 6 and 7 are noted below the sequence. T613 and S631 are marked in the 2-D diagram. **(B)** and **(C)** Percent change in current amplitude measured at 0 mV (WT or WT-like) or +60 mV (mutant) induced by 20 uM PD or 30 uM NS plotted against the channel types along the abscissa in (C), where Cys side chains modified by disulfide bonding (-S-S-) or MTSET modification (+MTS) are noted. Hatched histogram bars for WT or WT-like channel phenotype are shown in white background, while those for mutant phenotype are shown in black background (*inset* in 'C'). **(D)** Superimposed current traces recorded from oocytes expressing the specified hERG mutants. Currents were elicited by the voltage clamp protocol diagrammed on top under 3 conditions: control (light gray traces), after adding 30 uM NS (dark gray traces), and after adding 20 uM PD in the continuous presence of NS (black traces).

Fig. 7 Modifications of Cys side chains introduced into 2 pore entrance positions differentially impacted on the 'activator' effects of PD307243 and NS1643. *C*urrents were elicited by different voltage clamp protocols to (a) illustrate their gating behavior as WT-like or Mutant, and (b) probe for drug effects on both outward and inward currents through the channels. For the sake of simplicity, individual voltage clamp protocols are not shown; only the step voltages are noted (holding voltage was -80 mV in all cases). **(A)** T613C manifested WT-like gating behavior under the control conditions (gray trace), and switched to the mutant behavior after MTSET modification (black trace). **(B)** S631C manifested WT-like behavior (gray

Molecular Pharmacology Fast Forward. Published on March 27, 2008 as DOI: 10.1124/mol.108.045591
This article has not been copyedited and formatted. The final version may differ from this version.

trace) when DTT treated, but switched to Mutant behavior (black trace) after H_2O_2 treatment with pulsing. **(C)** and **(D)** PD was effective in increasing currents through the T613C and S631C channels in both WT-like and mutant behavior. On the other hand, NS was effective in increasing currents through the T613C and S631C channels in the WT-like mode, but incapable of increasing currents when the channels were in the mutant mode.

Fig. 8 BeKm-1 potentiated the activator effect of PD307243 but suppressed the activator effect of NS1643. (A) Cartoon of hERG pore domain with an extracellular BeKm-1 structure. Three hERG subunits are depicted, with the fourth one closest to viewers removed to reveal the narrow selectivity filter and wide inner cavity of the pore. Cylinders represent the S5-P helices. **(B)** *Main plot*: Two time courses of changes in hERG current amplitude before and after exposure to PD 20 uM. Current amplitudes were measured from time-dependent currents during 1-s steps to 0 mV and normalized by the current right before PD application. One experiment (open symbols) was conducted in the absence of BeKm-1. The other (black symbols) was conducted in the presence of 10 uM BeKm-1. *Inset*: The complete time course of the second experiment: BeKm-1 suppressed the current by 80% and subsequent application of PD in the continuous presence of BeKm-1 effectively increased the current amplitude. **(C)** NS (30 uM) effect on hERG in the absence or presence of BeKm-1. The format is the same as that of (B). **(D)** Data summary. * $p < 0.05$, data obtained in the presence of BeKm-1 vs those without BeKm-1.

Fig. 9 An outer pore blocker, tetrapentylammonium cation ($TPeA^+$) or an inner cavity blocker, dofetilide (DOF) prevented the activator effect of PD307243 on hERG. (A) Cartoon of a $TPeA^+$ ion binding to the outer pore entrance of hERG. **(B)** Time course of changes in

Molecular Pharmacology Fast Forward. Published on March 27, 2008 as DOI: 10.1124/mol.108.045591
This article has not been copyedited and formatted. The final version may differ from this version.

hERG current amplitude before and after application of 50 uM $TPeA^+$, and after application of increasing concentrations of PD in the continuous presence of $TPeA^+$. Current amplitudes were measured from time-dependent currents during 1-s step to 0 mV and normalized by control. *Inset*: Summary of PD (20 uM)-induced changes in hERG current amplitude in the absence or presence of $TPeA^+$. **(C)** and **(D)** The format is the same as that in (A) and (B). DOF binds from the intracellular side of the membrane to the inner cavity.

Fig. 10 Agonist effect of PD307243 on native I_{Kr} in a guinea pig ventricular myocyte. Shown are superimposed current traces recorded from the same myocyte before (thin gray trace) and 5 min after application of PD 10 uM (thick black trace). Currents were elicited by the pulse protocol diagrammed**.** Based on the difference in voltage-dependence of activation (Sanguinetti and Jurkiewicz1990), time-dependent current during the -10 mV step and the following tail current at -50 mV mainly represented I_{Kr}. Time-dependent current during the +50 mV step mainly represented I_{Ks} although the following tail current resulted from both I_{Kr} and I_{Ks}.

Molecular Pharmacology Fast Forward. Published on March 27, 2008 as DOI: 10.1124/mol.108.045591
This article has not been copyedited and formatted. The final version may differ from this version.

Table 1 Parameter values used in kinetic model[a] simulation of the effects of PD(307243) and NS(1643) on the hERG channel

Parameter	Unit	Control	PD[b]	NS[c]
$\alpha_{ao}(0)$	s^{-1}	22.3	22.3	22.3
z_{ao}		0.294	0.294	0.294
$\beta_{oa}(0)$	s^{-1}	0.047	0.047	0.047
z_{bo}		-1.577	-1.577	-1.577
κ_f	s^{-1}	23.8	23.8	23.8
κ_b	s^{-1}	36.8	36.8	36.8
$\alpha_{a1}(0)$	s^{-1}	13.7	13.7	**54.9**
z_{a1}		0.955	0.955	0.955
$\beta_{a1}(0)$	s^{-1}	0.069	0.069	**0.017**
z_{b1}		-1.045	-1.045	-1.045
$\alpha_i(0)$	s^{-1}	90.8	**45.4**	**45.4**
z_{ai}		0.585	0.585	0.585
$\beta_i(0)$	s^{-1}	6.5	6.5	6.5
z_{bi}		-0.817	-0.817	-0.817

a. The kinetic model of hERG gating was based on that of Wang et al (1997):

$$\mathbf{C_0} \underset{\beta_{ao}}{\overset{\alpha_{ao}}{\rightleftharpoons}} \mathbf{C_1} \underset{\kappa_b}{\overset{\kappa_f}{\rightleftharpoons}} \mathbf{C_2} \underset{\beta_{a1}}{\overset{\alpha_{a1}}{\rightleftharpoons}} \mathbf{O} \underset{\beta_i}{\overset{\alpha_i}{\rightleftharpoons}} \mathbf{I}$$

Molecular Pharmacology Fast Forward. Published on March 27, 2008 as DOI: 10.1124/mol.108.045591
This article has not been copyedited and formatted. The final version may differ from this version.

where C_x, O, and I represent closed states, open state and inactivated state, respectively. The transitions between C_o and C_1, C_2 and O, as well as O and I are voltage-dependent, with rate constants calculated as shown below:

$\alpha_{a0}(V) = \alpha_{ao}(0)*\exp(z_{ao}VF/RT)$ $\beta_{a0}(V) = \beta_{ao}(0)*\exp(z_{bo}VF/RT)$

$\alpha_{a1}(V) = \alpha_{a1}(0)*\exp(z_{a1}VF/RT)$ $\beta_{a1}(V) = \beta_{a1}(0)*\exp(z_{b1}VF/RT)$

$\alpha_{i}(V) = \alpha_{i}(0)*\exp(z_{ai}VF/RT)$ $\beta_{i}(V) = \beta_{i}(0)*\exp(z_{bi}VF/RT)$

where $\alpha_x(V)$ and $\alpha_x(0)$ are forward (or right-ward according to the model) rate constants at voltages of 'V' and 0 mV, respectively, and z_{ax} is the equivalent gating charge involved in the gating transition; $\beta_x(V)$, $\beta_x(0)$ and z_{bx} are the corresponding parameters for the backward or left-ward transitions. The transition between C_1 and C_2 is voltage-independent, with forward and backward rate constants of κ_f and κ_b respectively.

b. The only change in parameter values for PD simulation was a 50% reduction in the 'O' to 'I' transition rate (highlighted in **bold**).

c. The changes in parameter values for NS simulation included: 50% reduction in the 'O' to 'I' transition rate, a 4-fold increase in the 'C_2' to 'O' transition rate, and a 75% reduction in 'O' to 'C_2' transition rate (highlighted in **bold**).

$$K_d = K_{on}/K_{off}$$

Fig. 1

Fig. 2

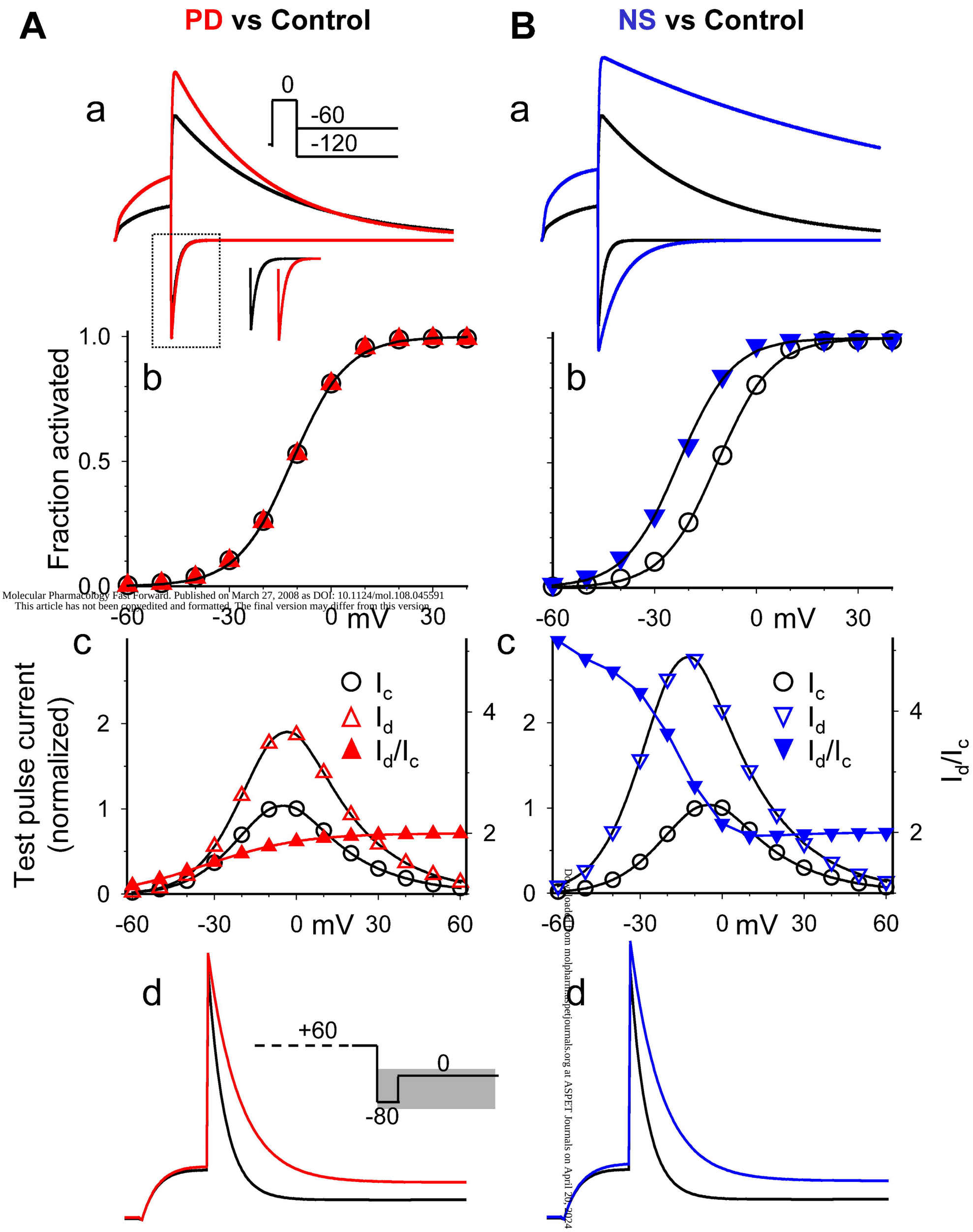

Molecular Pharmacology Fast Forward. Published on March 27, 2008 as DOI: 10.1124/mol.108.045591
This article has not been copyedited and formatted. The final version may differ from this version.

Fig. 3

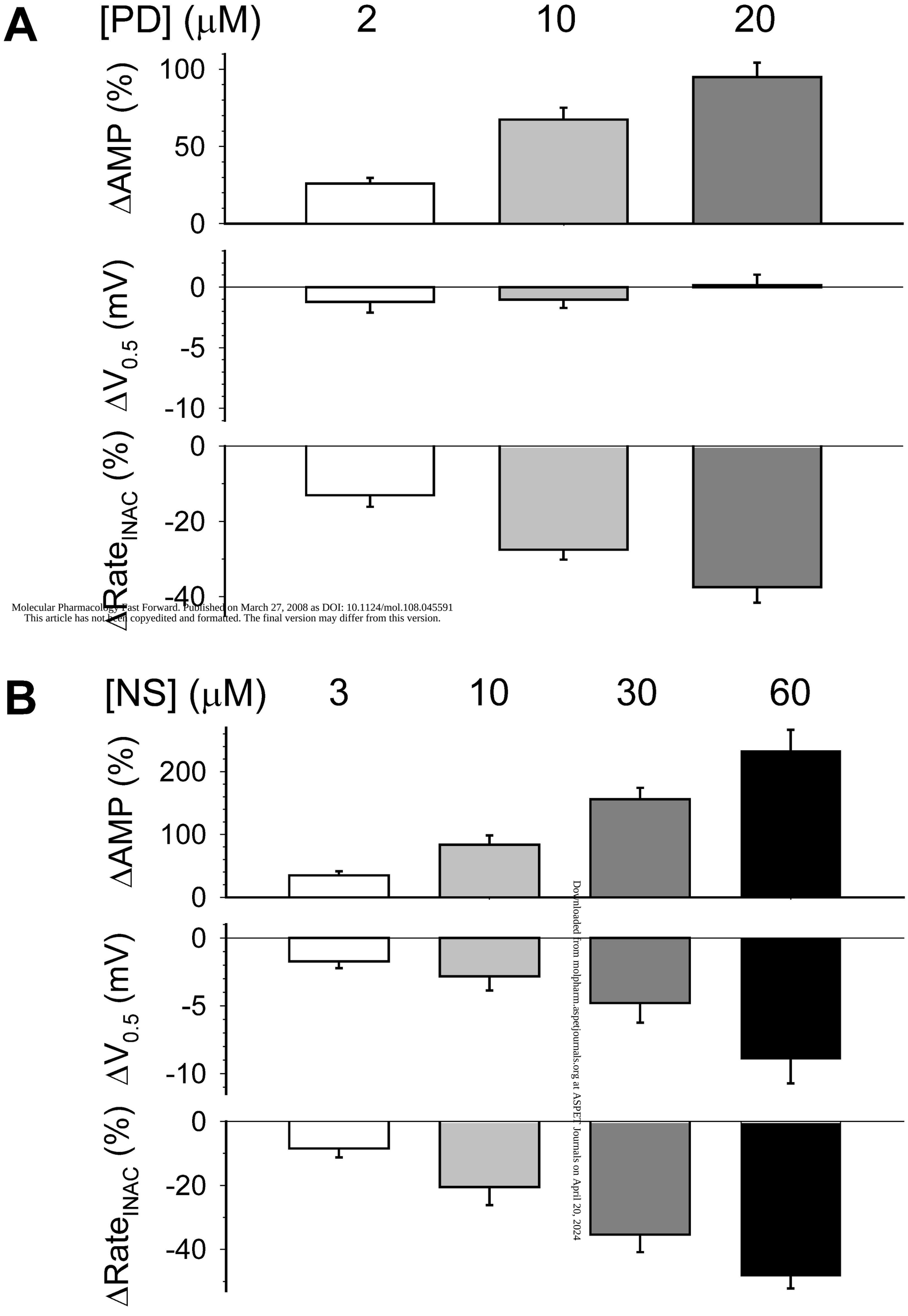

Molecular Pharmacology Fast Forward. Published on March 27, 2008 as DOI: 10.1124/mol.108.045591
This article has not been copyedited and formatted. The final version may differ from this version.

Fig. 4

Fig. 5

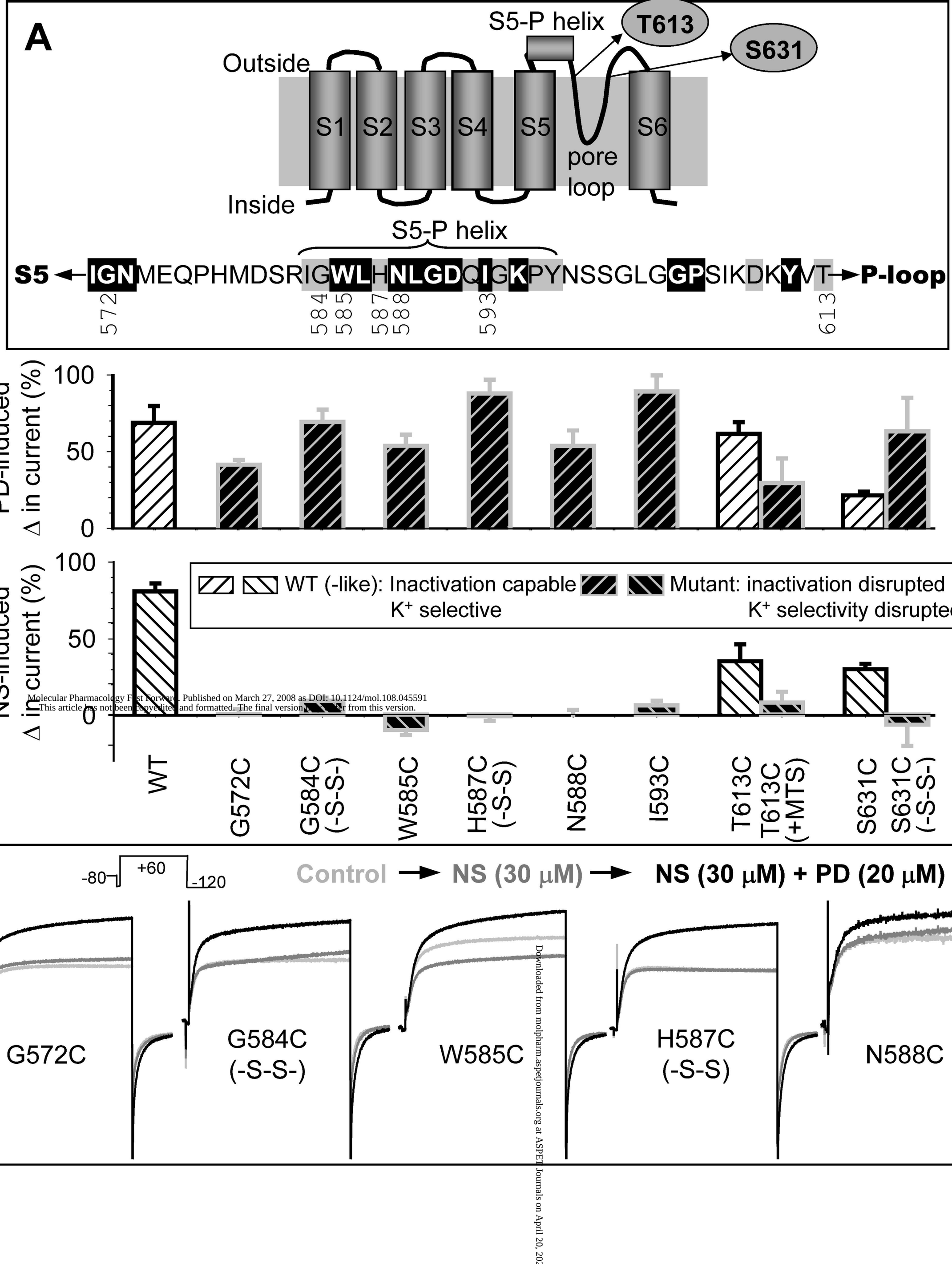

Fig. 6

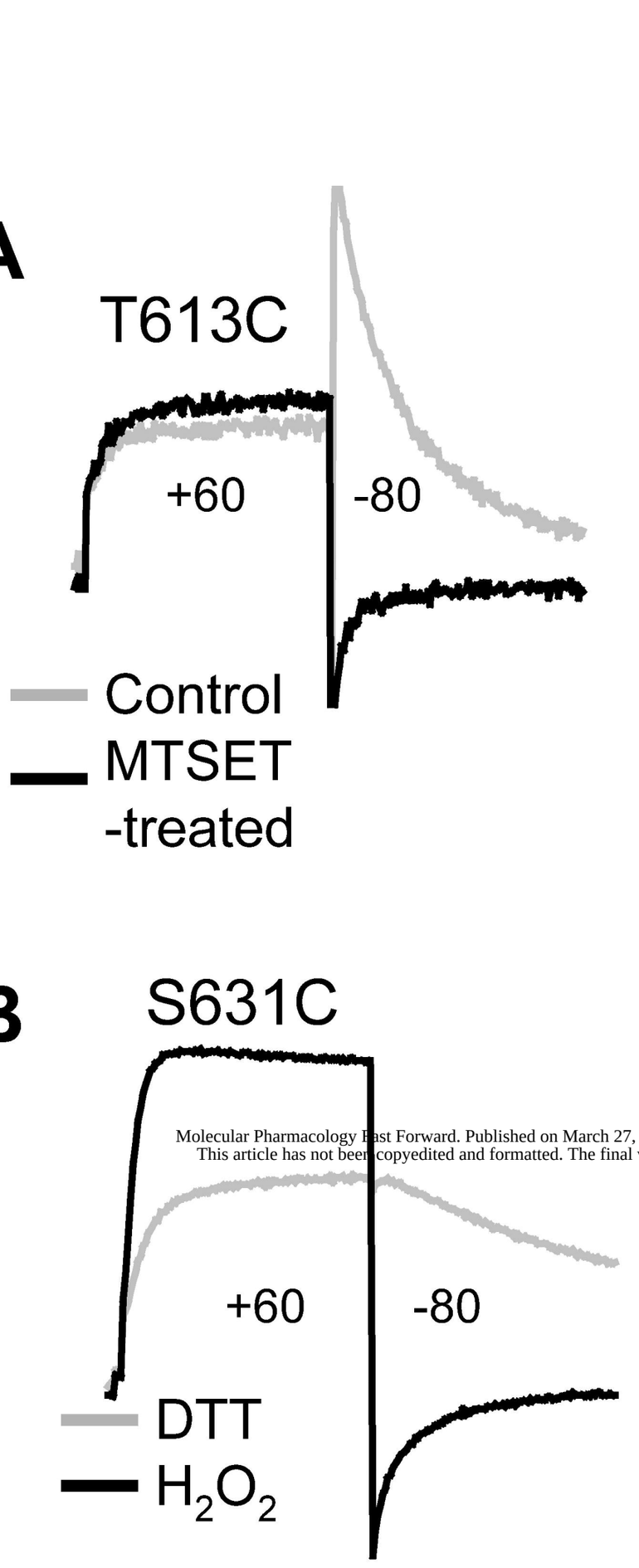

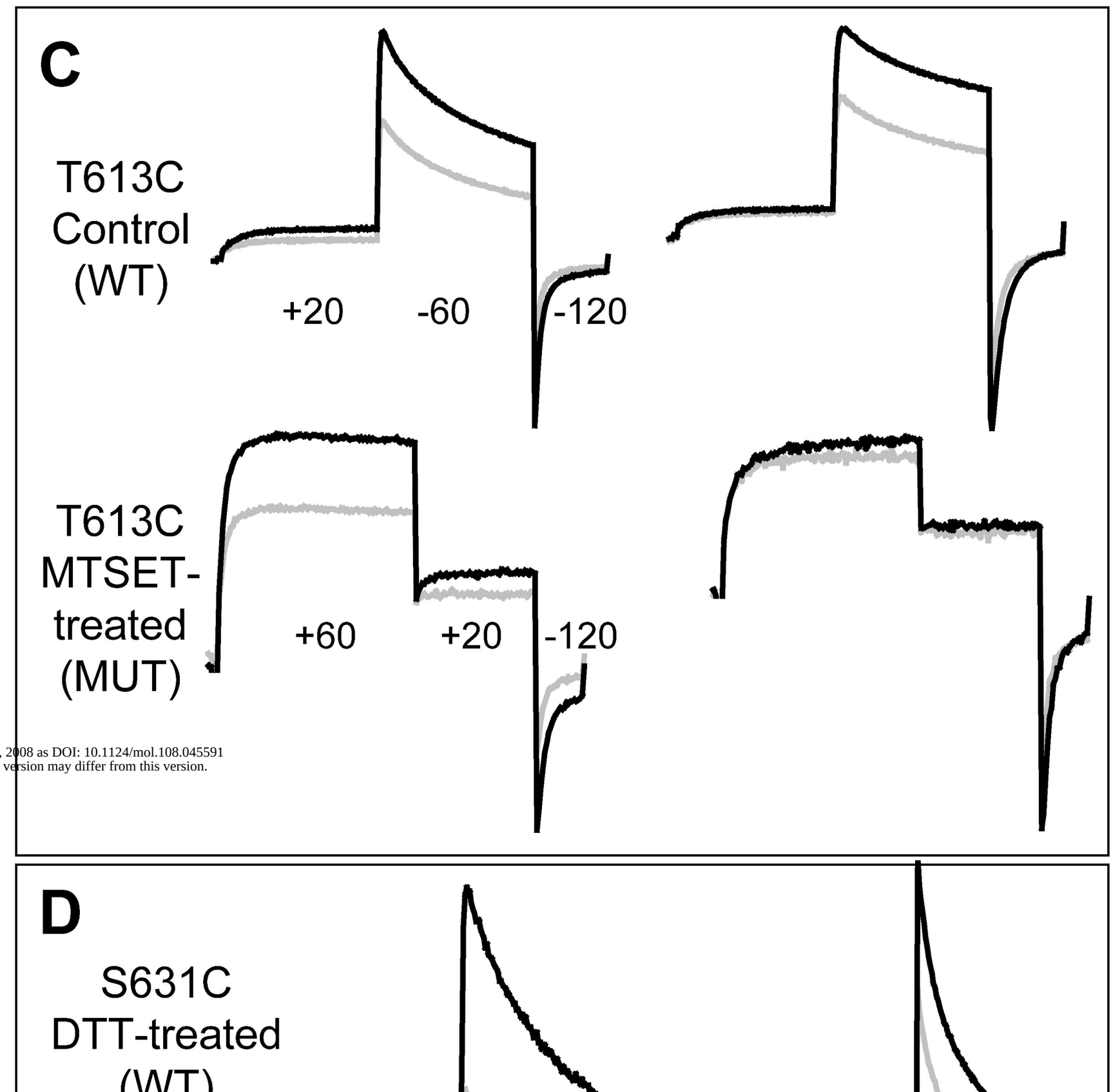

Fig. 7

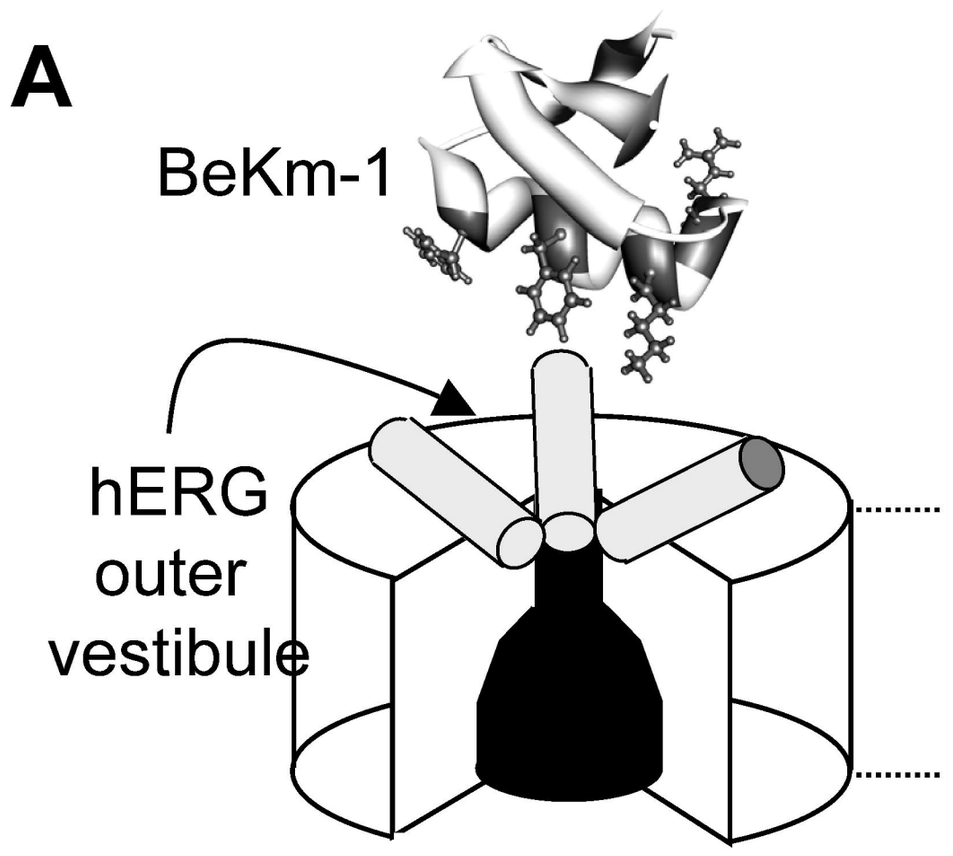

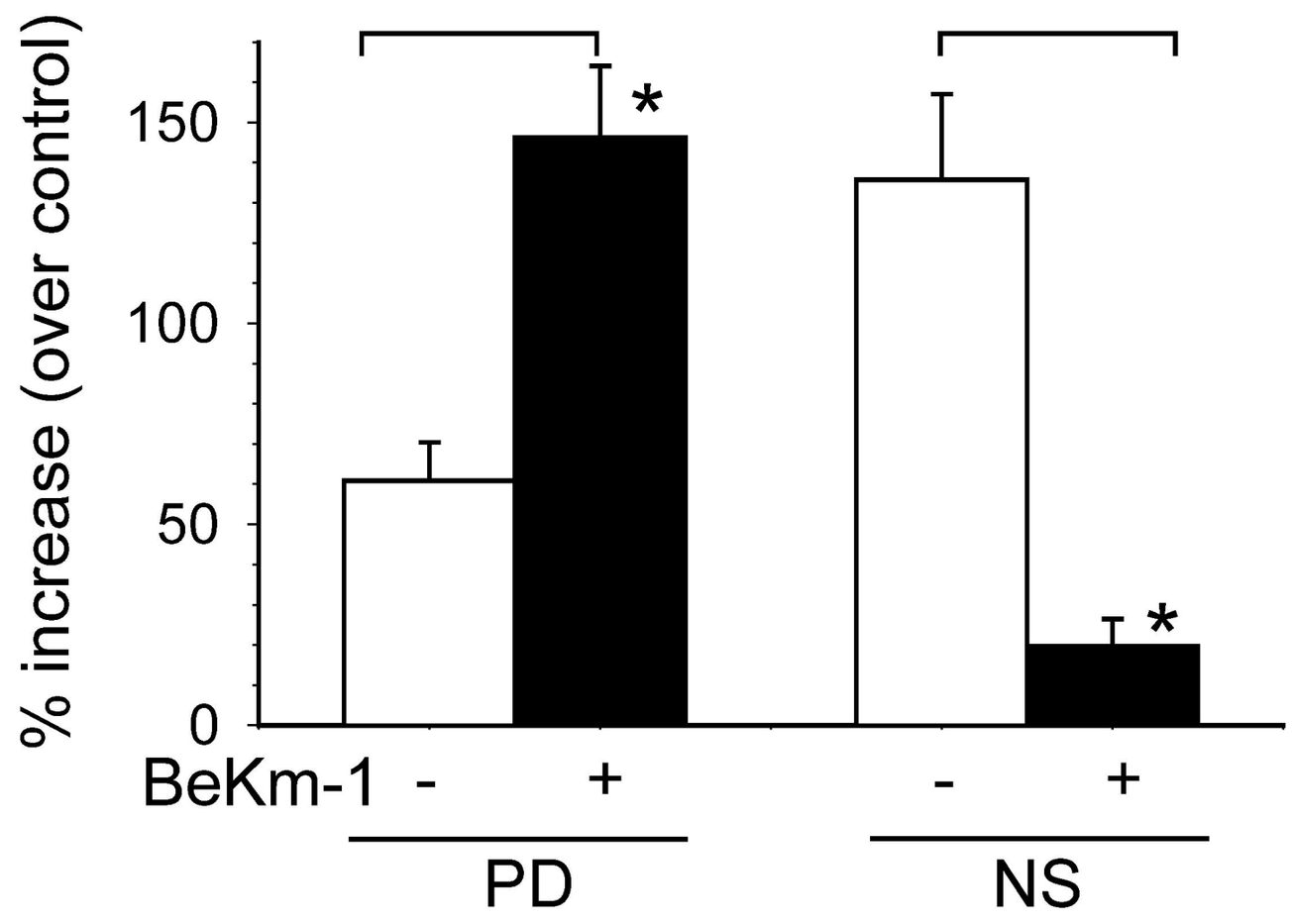

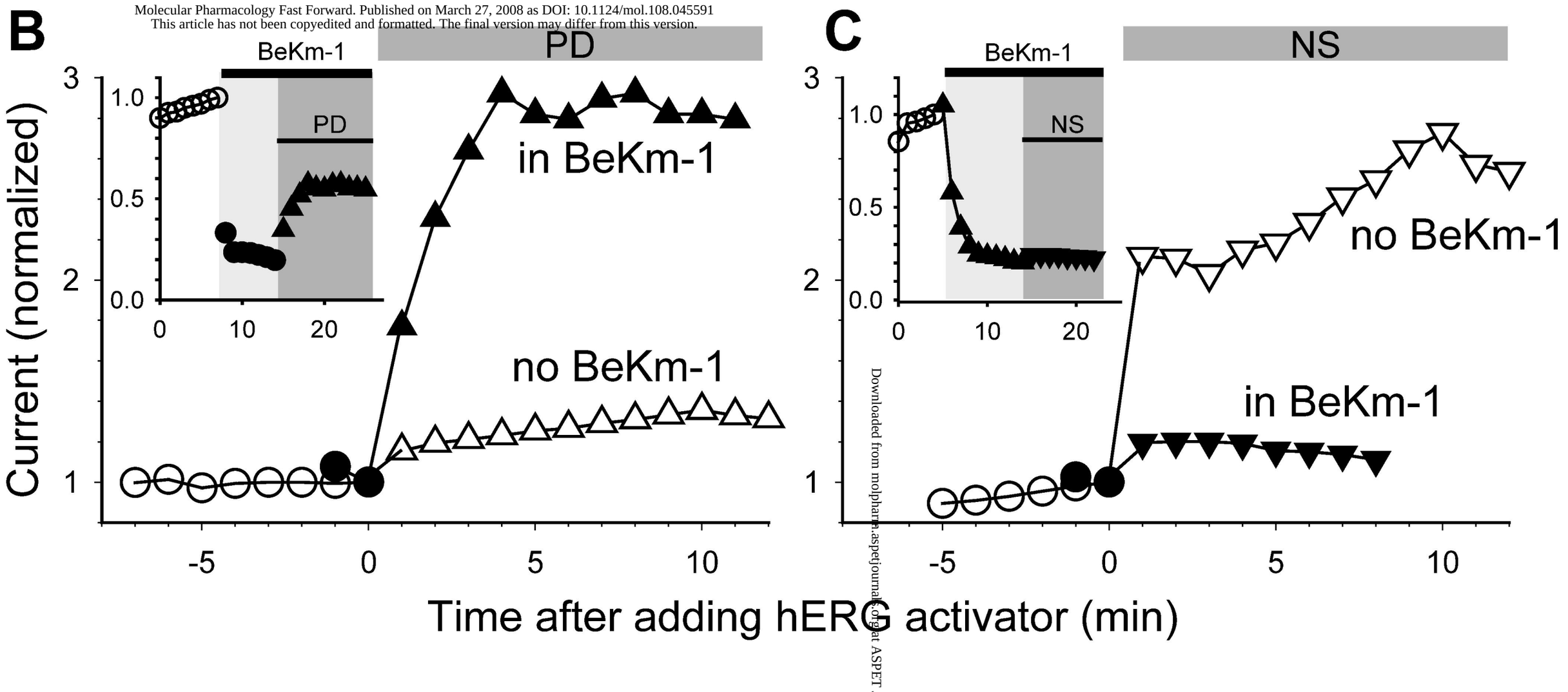

Fig. 8

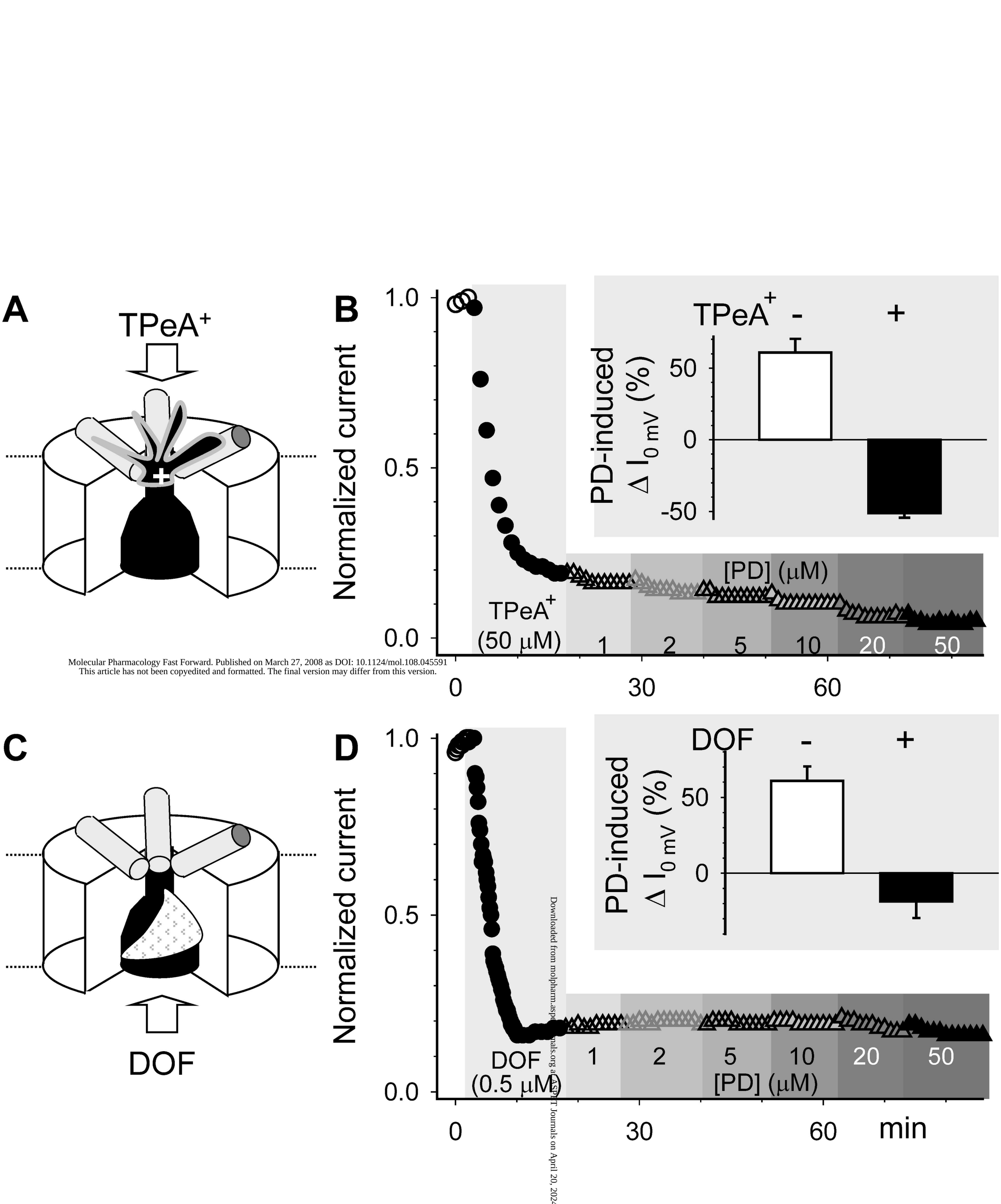

Fig. 9

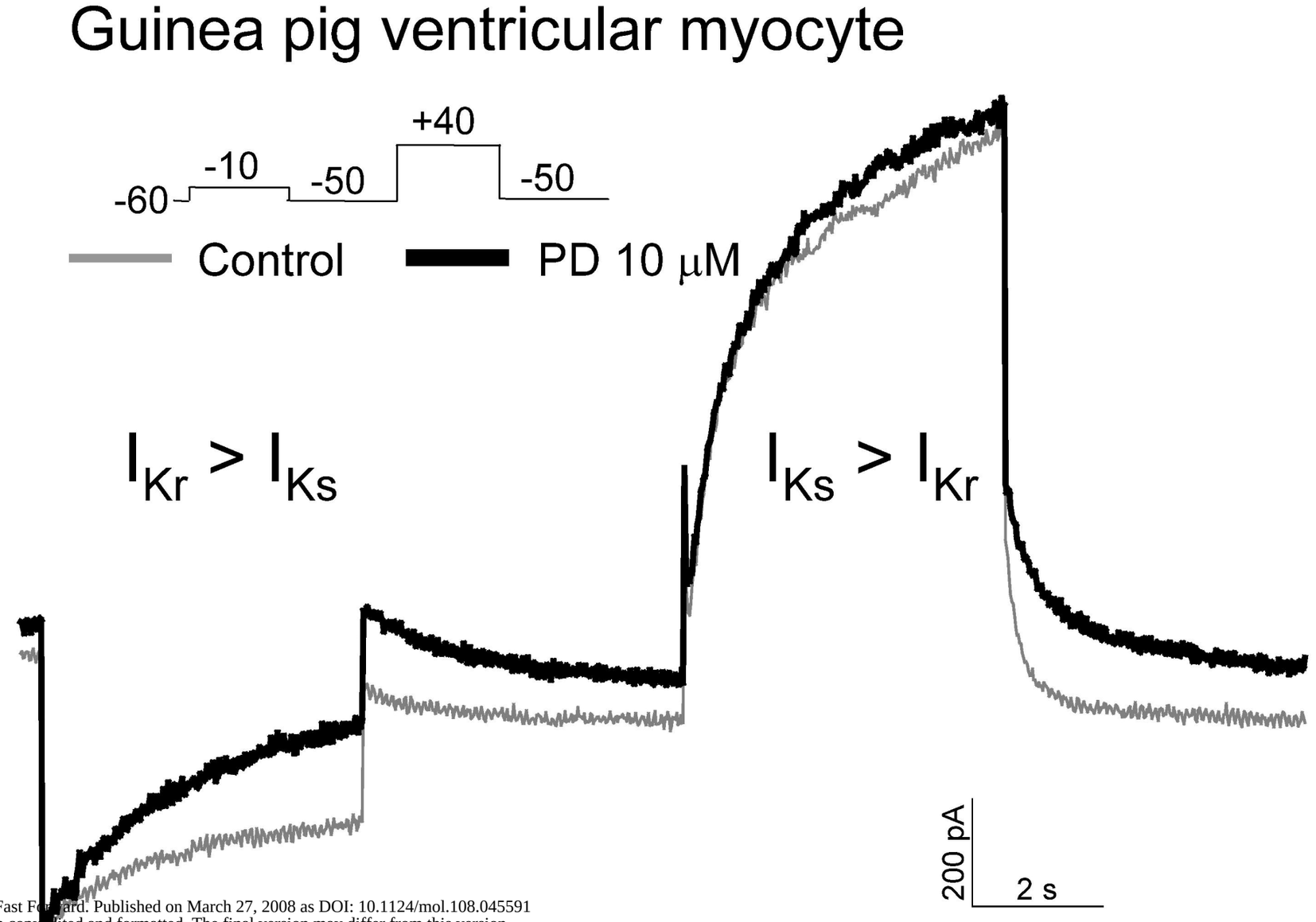

Fig. 10